Valentina De Romeri

(IFIC Valencia - UV/CSIC)

# New Physics Searches with Neutrino Experiments

5th IBS-IFT-MultiDark Workshop

(Dark World to Swampland)

16 October 2020

Mainly based on Phys. Rev. D98 (2018) 07501 and JHEP 08 (2020) 018

# Outline

1) Neutrino physics
   - Current status of neutrino global fits

2) Neutrino quantum decoherence
   - Distance-dependent loss of coherence
   - Probes of neutrino quantum decoherence at reactors

3) Coherent Elastic Neutrino-Nucleus Scattering (CE$\nu$NS)
   - Observation of CE$\nu$NS with COHERENT
   - Neutrino generalised interactions (NGI)
   - COHERENT constraints on NGI

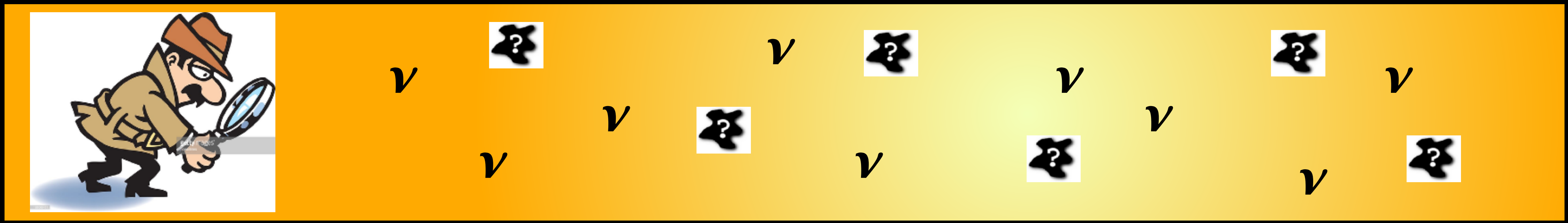

# Lepton mixing and neutrino physics

- As of today, data favour a three-active neutrinos oscillation framework.

- Neutrino oscillation parameters have been inferred by detecting neutrinos coming from the Sun, the Earth's atmosphere, nuclear reactors and accelerator beams.

| parameter | best fit $\pm 1\sigma$ | $2\sigma$ range | $3\sigma$ range |
|---|---|---|---|
| $\Delta m^2_{21} [10^{-5}\mathrm{eV}^2]$ | $7.50^{+0.22}_{-0.20}$ | 7.11–7.93 | 6.94–8.14 |
| $\lvert\Delta m^2_{31}\rvert [10^{-3}\mathrm{eV}^2]$ (NO) | $2.56^{+0.03}_{-0.04}$ | 2.49–2.62 | 2.46–2.65 |
| $\lvert\Delta m^2_{31}\rvert [10^{-3}\mathrm{eV}^2]$ (IO) | $2.46 \pm 0.03$ | 2.40–2.52 | 2.37–2.55 |
| $\sin^2\theta_{12}/10^{-1}$ | $3.18 \pm 0.16$ | 2.86–3.52 | 2.71–3.70 |
| $\theta_{12}/^\circ$ | $34.3 \pm 1.0$ | 32.3–36.4 | 31.4–37.4 |
| $\sin^2\theta_{23}/10^{-1}$ (NO) | $5.66^{+0.16}_{-0.22}$ | 5.05–5.96 | 4.41–6.09 |
| $\theta_{23}/^\circ$ (NO) | $48.79^{+0.93}_{-1.25}$ | 45.26–50.56 | 41.63–51.32 |
| $\sin^2\theta_{23}/10^{-1}$ (IO) | $5.66^{+0.18}_{-0.23}$ | 5.14–5.97 | 4.46–6.09 |
| $\theta_{23}/^\circ$ (IO) | $48.79^{+1.04}_{-1.30}$ | 45.78–50.59 | 41.88–51.30 |
| $\sin^2\theta_{13}/10^{-2}$ (NO) | $2.225^{+0.055}_{-0.078}$ | 2.081–2.349 | 2.015–2.417 |
| $\theta_{13}/^\circ$ (NO) | $8.58^{+0.11}_{-0.15}$ | 8.30–8.82 | 8.16–8.94 |
| $\sin^2\theta_{13}/10^{-2}$ (IO) | $2.250^{+0.056}_{-0.076}$ | 2.107–2.373 | 2.039–2.441 |
| $\theta_{13}/^\circ$ (IO) | $8.63^{+0.11}_{-0.15}$ | 8.35–8.86 | 8.21–8.99 |
| $\delta/\pi$ (NO) | $1.20^{+0.23}_{-0.14}$ | 0.93–1.80 | 0.80–2.00 |
| $\delta/^\circ$ (NO) | $216^{+41}_{-25}$ | 168–325 | 144–360 |
| $\delta/\pi$ (IO) | $1.54 \pm 0.13$ | 1.27–1.79 | 1.14–1.90 |
| $\delta/^\circ$ (IO) | $277^{+23}_{-24}$ | 229–322 | 205–342 |

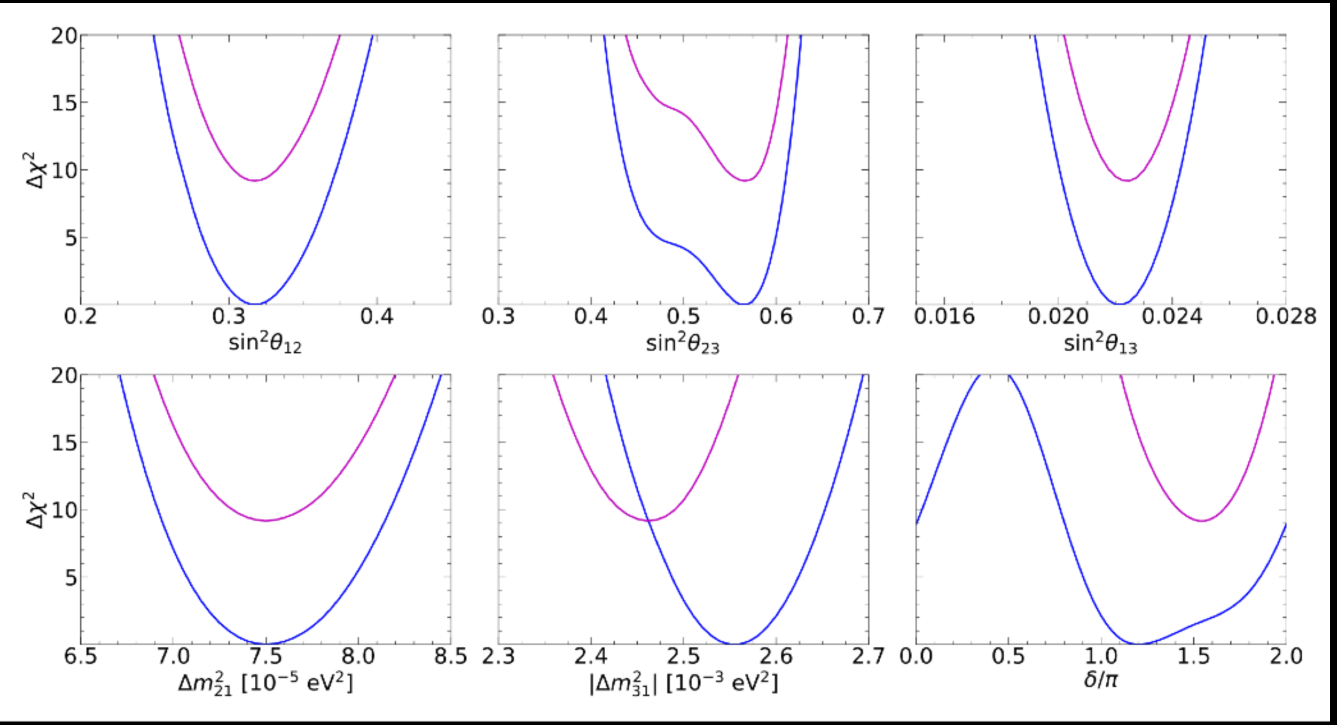


arXiv:2006.11237 P.F. de Salas et al.,
https://globalfit.astroparticles.es/

# Lepton mixing and neutrino physics

- very precise and robust determination for most of the mixing parameters
- slight preference for $\theta_{23}$ at the 2nd octant
- preference for $\pi < \delta < 2\pi$; CP conservation allowed at $1.4\sigma$ ($3.9\sigma$) for NO (IO)
- $\sim 3\sigma$ hint in favour of NO from atmospheric, LBL and reactor data

| parameter | best fit $\pm 1\sigma$ | $2\sigma$ range | $3\sigma$ range |
|---|---|---|---|
| $\Delta m^2_{21} [10^{-5}\text{eV}^2]$ | $7.50^{+0.22}_{-0.20}$ | 7.11–7.93 | 6.94–8.14 |
| $\|\Delta m^2_{31}\| [10^{-3}\text{eV}^2]$ (NO) | $2.56^{+0.03}_{-0.04}$ | 2.49–2.62 | 2.46–2.65 |
| $\|\Delta m^2_{31}\| [10^{-3}\text{eV}^2]$ (IO) | $2.46 \pm 0.03$ | 2.40–2.52 | 2.37–2.55 |
| $\sin^2\theta_{12}/10^{-1}$ | $3.18 \pm 0.16$ | 2.86–3.52 | 2.71–3.70 |
| $\theta_{12}/^\circ$ | $34.3 \pm 1.0$ | 32.3–36.4 | 31.4–37.4 |
| $\sin^2\theta_{23}/10^{-1}$ (NO) | $5.66^{+0.16}_{-0.22}$ | 5.05–5.96 | 4.41–6.09 |
| $\theta_{23}/^\circ$ (NO) | $48.79^{+0.93}_{-1.25}$ | 45.26–50.56 | 41.63–51.32 |
| $\sin^2\theta_{23}/10^{-1}$ (IO) | $5.66^{+0.18}_{-0.23}$ | 5.14–5.97 | 4.46–6.09 |
| $\theta_{23}/^\circ$ (IO) | $48.79^{+1.04}_{-1.30}$ | 45.78–50.59 | 41.88–51.30 |
| $\sin^2\theta_{13}/10^{-2}$ (NO) | $2.225^{+0.055}_{-0.078}$ | 2.081–2.349 | 2.015–2.417 |
| $\theta_{13}/^\circ$ (NO) | $8.58^{+0.11}_{-0.15}$ | 8.30–8.82 | 8.16–8.94 |
| $\sin^2\theta_{13}/10^{-2}$ (IO) | $2.250^{+0.056}_{-0.076}$ | 2.107–2.373 | 2.039–2.441 |
| $\theta_{13}/^\circ$ (IO) | $8.63^{+0.11}_{-0.15}$ | 8.35–8.86 | 8.21–8.99 |
| $\delta/\pi$ (NO) | $1.20^{+0.23}_{-0.14}$ | 0.93–1.80 | 0.80–2.00 |
| $\delta/^\circ$ (NO) | $216^{+41}_{-25}$ | 168–325 | 144–360 |
| $\delta/\pi$ (IO) | $1.54 \pm 0.13$ | 1.27–1.79 | 1.14–1.90 |
| $\delta/^\circ$ (IO) | $277^{+23}_{-24}$ | 229–322 | 205–342 |

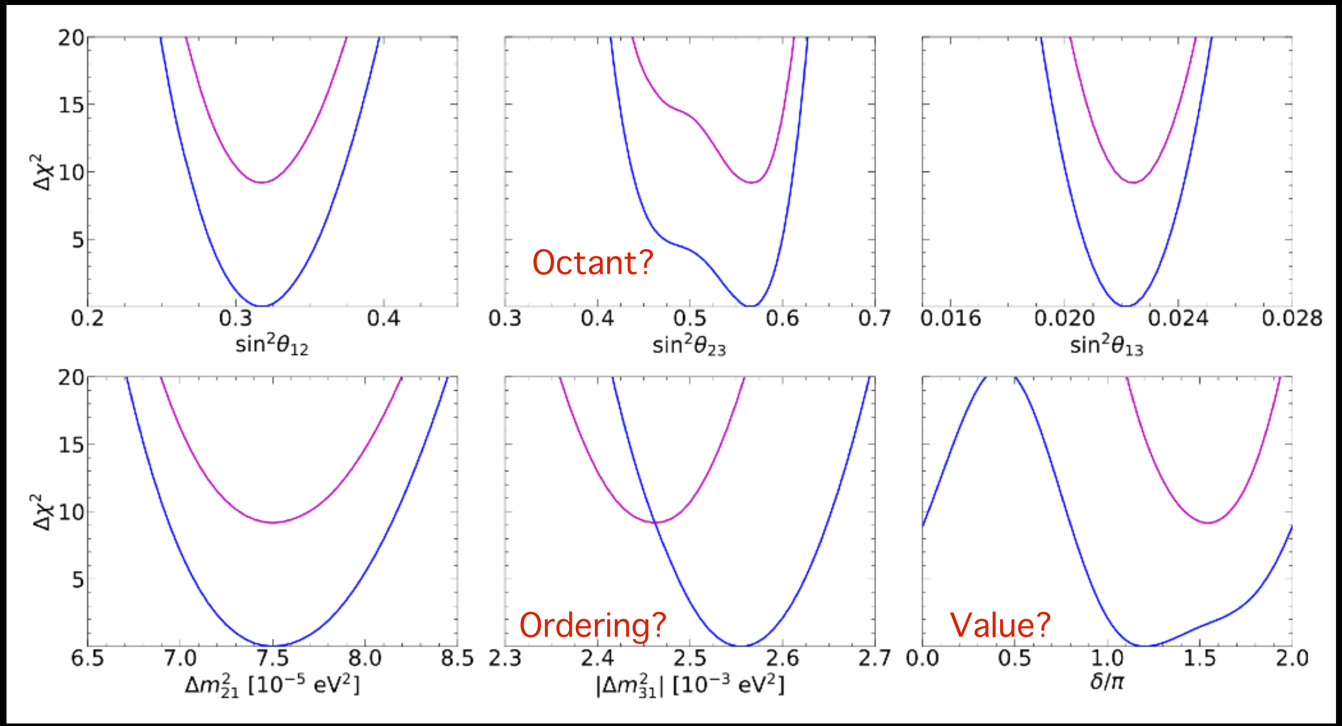


arXiv:2006.11237 P.F. de Salas et al.,
https://globalfit.astroparticles.es/

# Lepton mixing and neutrino physics

- very precise and robust determination for most of the mixing parameters
- slight preference for $\theta_{23}$ at the 2nd octant
- preference for $\pi < \delta < 2\pi$; CP conservation allowed at 1.4σ (3.9σ) for NO (IO)
- ~3σ hint in favour of NO from atmospheric, LBL and reactor data

| parameter | best fit $\pm 1\sigma$ | $2\sigma$ range | $3\sigma$ range |
|---|---|---|---|
| $\Delta m^2_{21} [10^{-5}\mathrm{eV}^2]$ | $7.50^{+0.22}_{-0.20}$ | 7.11–7.93 | 6.94–8.14 |
| $\|\Delta m^2_{31}\| [10^{-3}\mathrm{eV}^2]$ (NO) | $2.56^{+0.03}_{-0.04}$ | 2.49–2.62 | 2.46–2.65 |
| $\|\Delta m^2_{31}\| [10^{-3}\mathrm{eV}^2]$ (IO) | $2.46 \pm 0.03$ | 2.40–2.52 | 2.37–2.55 |
| $\sin^2\theta_{12}/10^{-1}$ | $3.18 \pm 0.16$ | 2.86–3.52 | 2.71–3.70 |
| $\theta_{12}/^\circ$ | $34.3 \pm 1.0$ | 32.3–36.4 | 31.4–37.4 |
| $\sin^2\theta_{23}/10^{-1}$ (NO) | $5.66^{+0.16}_{-0.22}$ | 5.05–5.96 | 4.41–6.09 |
| $\theta_{23}/^\circ$ (NO) | $48.79^{+0.93}_{-1.25}$ | 45.26–50.56 | [illegible] |
| $\sin^2\theta_{23}/10^{-1}$ (IO) | [illegible] | 5.14–5.97 | 4.46–6.09 |
| $\theta_{23}/^\circ$ (IO) | [illegible] | [illegible] | 41.88–51.30 |
| $\sin^2\theta_{13}/10^{-2}$ (NO) | [illegible] | [illegible] | 2.015–2.417 |
| $\theta_{13}/^\circ$ (NO) | $8.58^{+0.11}_{-0.15}$ | 8.30–8.82 | [illegible] |
| $\sin^2\theta_{13}/10^{-2}$ (IO) | [illegible] | 2.107–2.373 | 2.039–2.441 |
| $\theta_{13}/^\circ$ (IO) | $8.63^{+0.11}_{-0.15}$ | 8.35–8.86 | 8.21–8.99 |
| $\delta/\pi$ (NO) | $1.20^{+0.23}_{-0.14}$ | 0.93–1.80 | 0.80–2.00 |
| $\delta/^\circ$ (NO) | $216^{+41}_{-25}$ | 168–325 | 144–360 |
| $\delta/\pi$ (IO) | $1.54 \pm 0.13$ | 1.27–1.79 | 1.14–1.90 |
| $\delta/^\circ$ (IO) | $277^{+23}_{-24}$ | 229–322 | 205–342 |

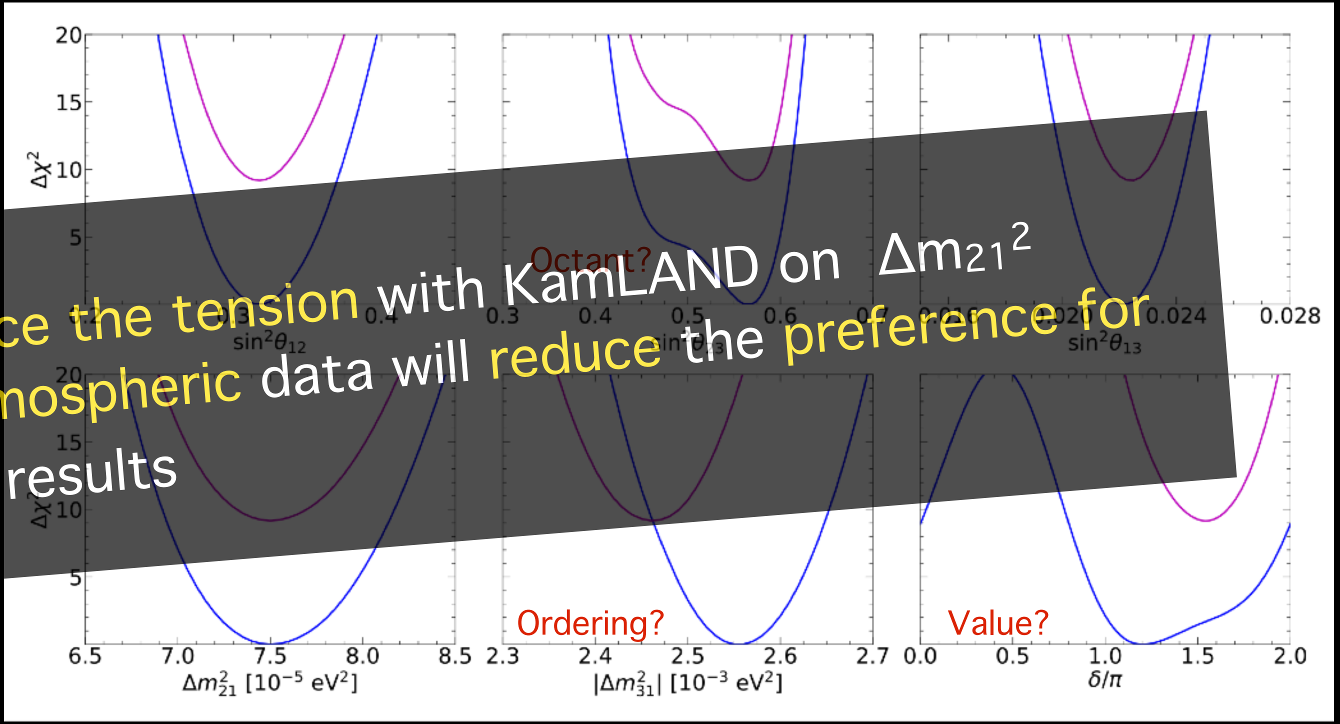


UPDATED ANALYSIS IN PROGRESS:

- new Super-K solar data will reduce the tension with KamLAND on $\Delta m_{21}{}^2$
- new T2K, NOvA and Super-K atmospheric data will reduce the preference for NO and affect δ and $\theta_{23}$ octant results

arXiv:2006.11237 P.F. de Salas et al.,
https://globalfit.astroparticles.es/

# Probing neutrino quantum decoherence at reactor experiments

A. de Gouvêa, V. De Romeri, C. A. Ternes, JHEP 08 (2020) 018

# Neutrino quantum decoherence

- Neutrino oscillations are an example of flavour oscillations, which arise when the particles produced and detected in an experiment are superpositions of different mass eigenstates.

- Consequence of the fact that the charged-current weak interactions are not diagonal in the basis of the mass eigenstates for both the charged leptons and the neutrinos.

- The QM uncertainty principle implies that when neutrinos are produced at some source they must be in a superposition of different momentum states. The neutrino wave function must be a wave packet.

- Coherence is essential for neutrino oscillations!


S. Nussinov, Phys. Lett. B 63 (1976) 201–203.
B. Kayser,, Phys. Rev. D 24 (1981) 110.
C. Giunti, C. Kim, and U. Lee, Phys. Rev. D 44 (1991) 3635–3640.
C. Giunti, C. Kim, and U. Lee, Phys. Lett. B 274 (1992) 87–94.
K. Kiers and N. Weiss, Phys. Rev. D 57 (1998) 3091–3105

C. Giunti and C. Kim, Phys. Rev. D 58 (1998) 017301,
W. Grimus, P. Stockinger, and S. Mohanty, Phys.
E. K. Akhmedov and J. Kopp, JHEP 04 (2010) 008
D. Naumov and V. Naumov, J. Phys. G 37 (2010) 105014
E. Akhmedov, D. Hernandez, and A. Smirnov, JHEP 04 (2012) 052

# Neutrino quantum decoherence

- To date there is no experimental evidence of distance-dependent loss of coherence for propagating neutrinos.

- Physics that leads to this type of decoherence: the wave packets corresponding to different neutrino mass eigenstates propagate with different speeds and, given enough time, the wave-packets ultimately separate.

- Eventually, the wave packets of two different mass eigenstates will have no significant overlap any more and their coherence will be lost, leading to a suppression of neutrino oscillations.

- Nuclear reactors are excellent laboratories to study neutrino coherence.

S. Nussinov, Phys. Lett. B 63 (1976) 201–203.
B. Kayser,, Phys. Rev. D 24 (1981) 110.
C. Giunti, C. Kim, and U. Lee, Phys.  Rev. D 44 (1991) 3635–3640.
C. Giunti, C. Kim, and U. Lee, Phys. Lett. B 274 (1992) 87–94.
K. Kiers and N. Weiss, Phys. Rev. D 57 (1998) 3091–3105
C. Giunti and C. Kim, Phys. Rev. D 58 (1998) 017301,
W. Grimus, P. Stockinger, and S. Mohanty, Phys.
E. K. Akhmedov and J. Kopp, JHEP 04 (2010) 008
D. Naumov and V. Naumov, J. Phys. G 37 (2010) 105014
E. Akhmedov, D. Hernandez, and A. Smirnov, JHEP 04 (2012) 052

# Decoherence and reactor experiments

- Jiangmen Underground Neutrino Observatory (JUNO)
  - 12 reactors
  - 1 far detector (+ 1 near detector under consideration)
  - JUNO will measure the solar parameters and the atmospheric mass splitting at below 1%
- Reactor Experiment for Neutrino Oscillation (RENO)
  - 6 power plants
  - 2 identical detectors
- Daya Bay reactor experiment
  - 6 power plants
  - 8 identical detectors at 3 experimental halls

# Neutrino oscillations with decoherence

The survival probability of electron antineutrinos including decoherence effects is:

$$P^{\mathrm{dec}}(\overline{\nu}_e \to \overline{\nu}_e) = \sum_{j,k} |U_{ej}|^2 |U_{ek}|^2 \exp[-i\Delta_{jk} - \xi_{jk}]$$

Giunti, Kim, Lee, PLB274 (1992)
M. Beuthe, PRD66 (2002)
Kayser, Kopp, arXiv:1005.4081

where $\Delta_{jk} \equiv 2\pi \frac{L}{L_{jk}^{\mathrm{osc}}} \equiv \frac{\Delta m_{jk}^2 L}{2E}$

and $\xi_{jk}(L,E) = \xi_{kj}(L,E)$ quantify the loss of coherence as a function of the neutrino energy and the baseline.

$$\xi_{jk}(L,E) = \left(\frac{L}{L_{jk}^{\mathrm{coh}}}\right)^2 \qquad L_{jk}^{\mathrm{coh}} = \frac{4\sqrt{2}E^2}{|\Delta m_{jk}^2|}\sigma$$

σ is the effective width of the neutrino wave-packet and depends on the spatial delocalisation of the neutrino source and of the detector.

# Decoherence effects at reactor experiments

Decoherence effects in reactor experiments grow with the baseline and decrease with the neutrino energy.

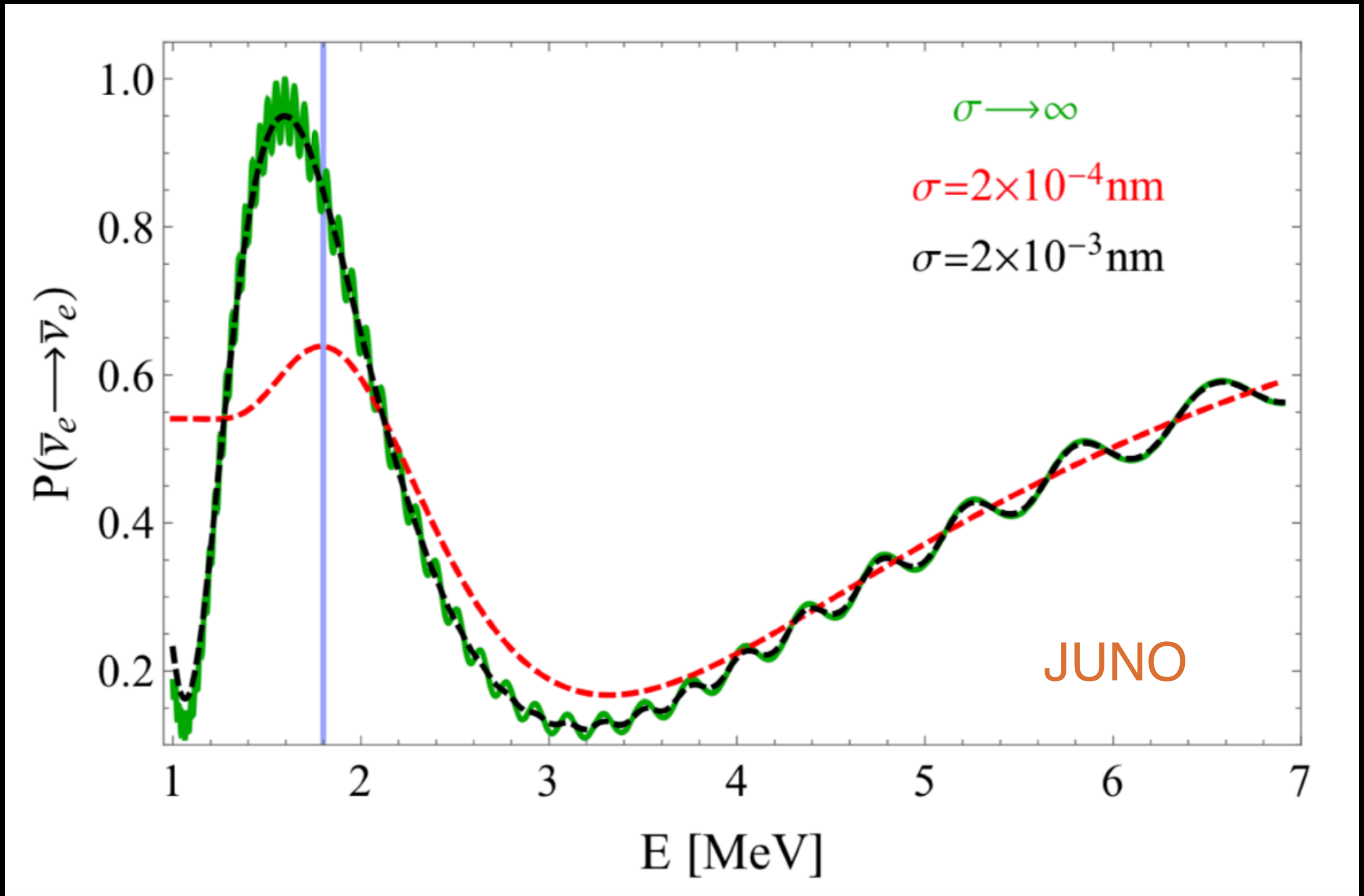


de Gouvêa, VDR, Ternes JHEP 08 (2020) 018

The fast oscillations "disappear" first and that the effect is more pronounced at smaller neutrino energies.

# Ruling out decoherence

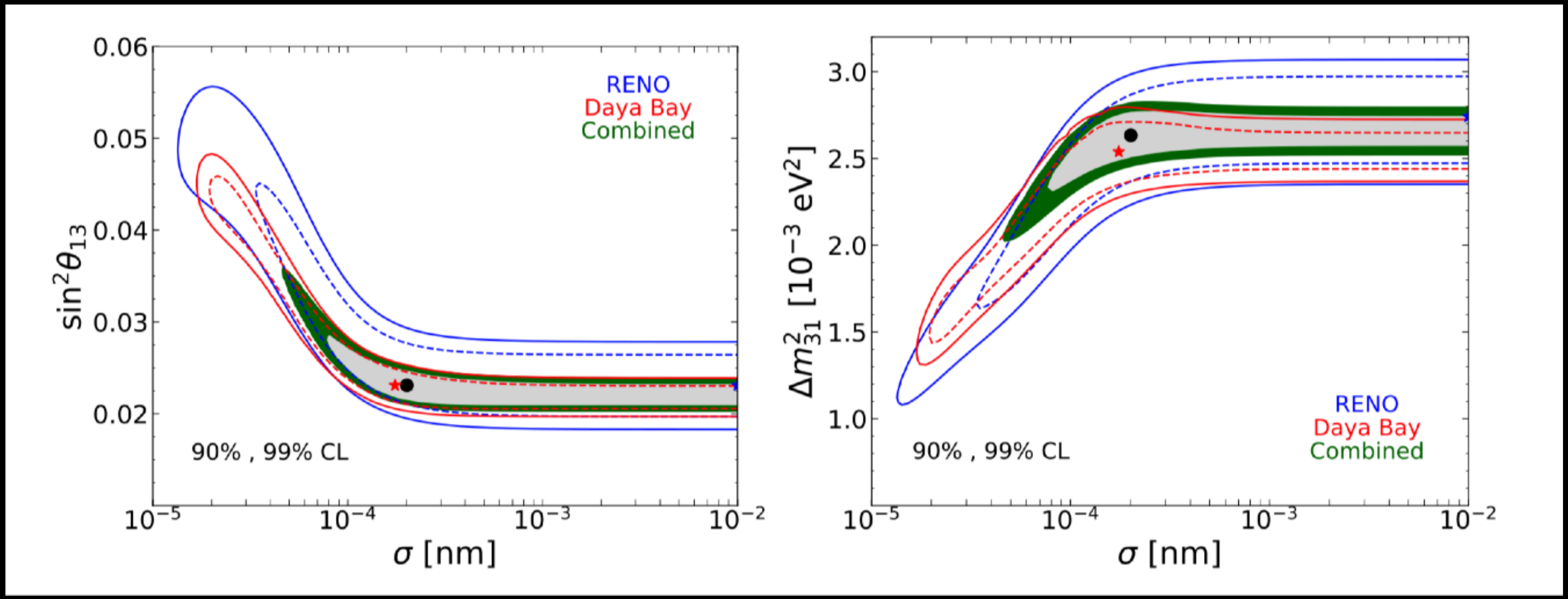


The reduction of sensitivity is due to a new correlation between the standard parameters and the wave packet width. Small values of sigma are correlated with large (small) values of the mixing angle (mass splitting).

de Gouvêa, VDR, Ternes JHEP 08 (2020) 018

The measurement of the standard neutrino oscillation parameters remains mostly unaffected when allowing for the possibility that σ is finite.

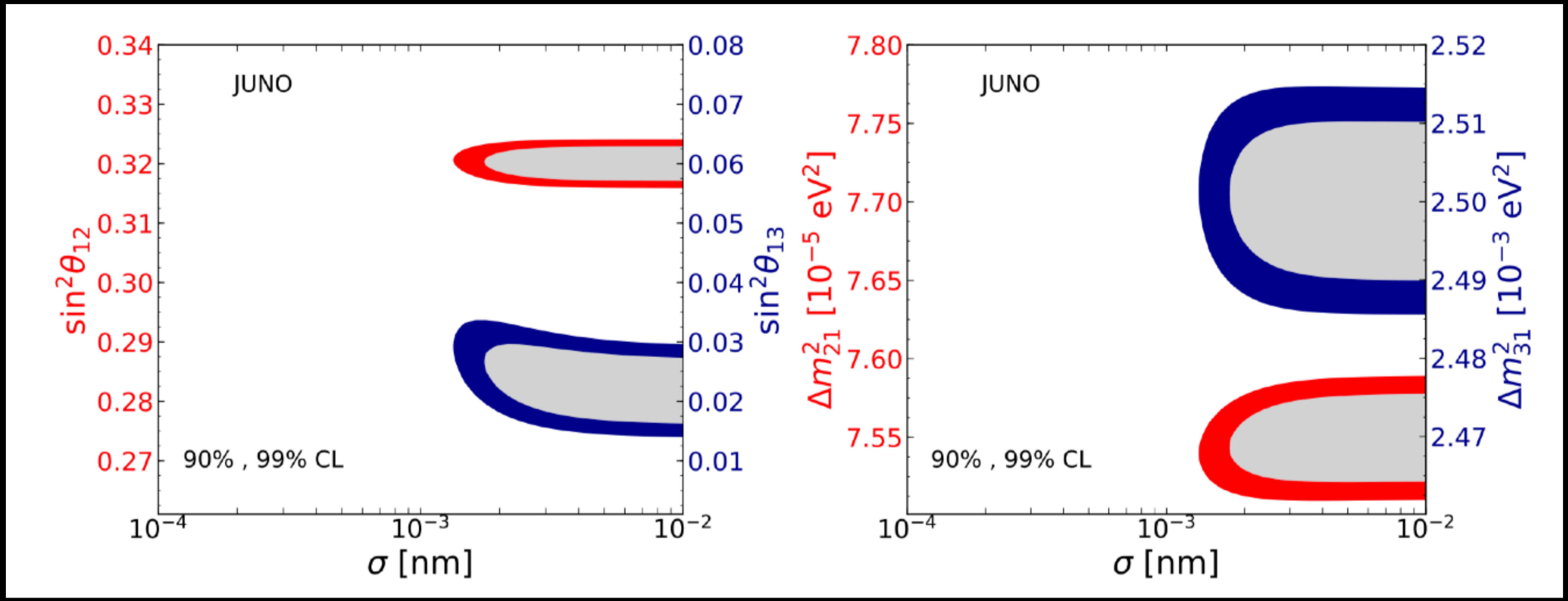

# Decoherence effects at reactor experiments

From the combined analysis RENO + DB we obtain a lower bound: σ > $10^{-4}$ nm at 90% CL. For larger values of sigma the effect in the oscillation probability disappears. With JUNO, a bound more than a factor 20 stronger than the current one can be obtained after 6 years of data taking.

The no-decoherence hypothesis would be excluded at more than 10 sigma.

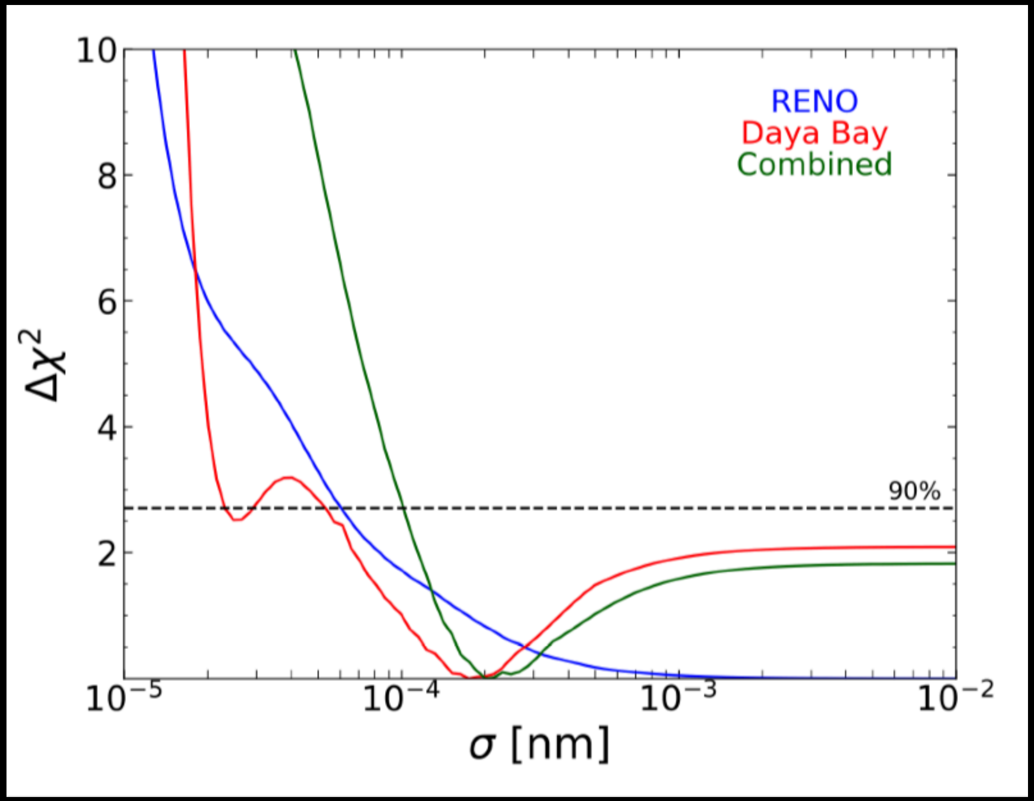


de Gouvêa, VDR, Ternes JHEP 08 (2020) 018

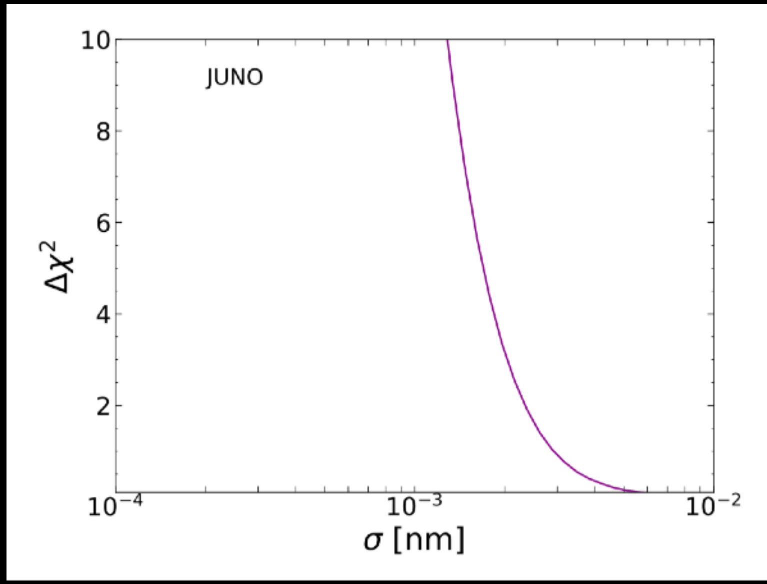


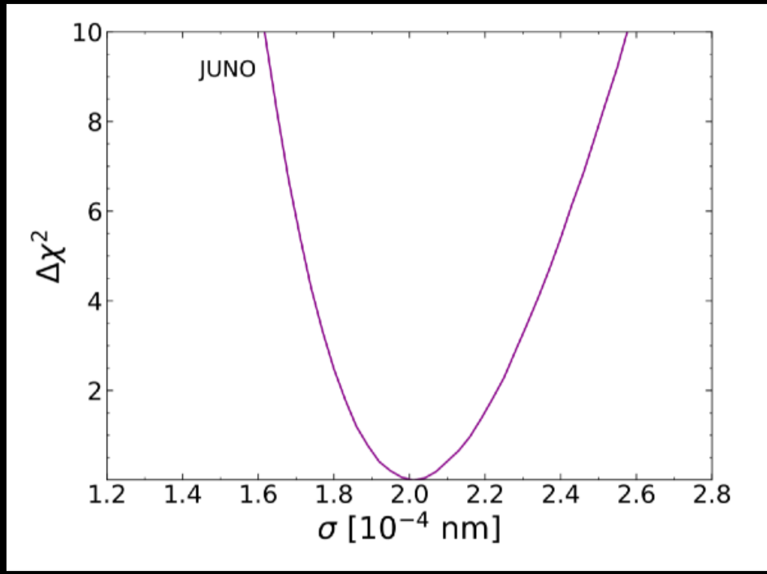

# Summary of decoherence effects

- The position-dependent loss of coherence of neutrinos produced and detected under any circumstances has never been observed.

- We have explored how well reactor antineutrino experiments can constrain or measure the loss of coherence of reactor antineutrinos.

- We found that current reactor data from Daya Bay and RENO constrain the neutrino wave-packet, $\sigma > 10^{-4}$ nm while future data from JUNO should be sensitive to $\sigma < 2.1 \times 10^{-3}$ nm.

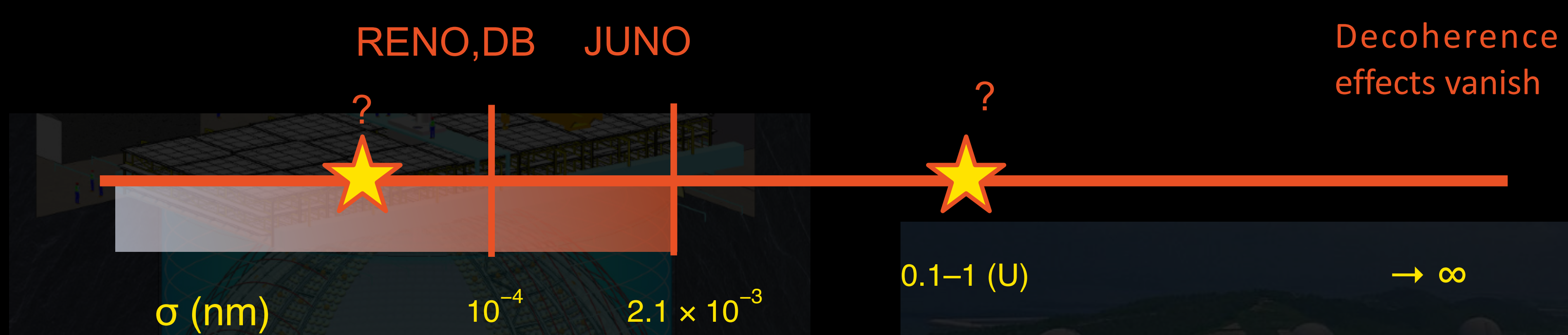


- The discovery of nontrivial decoherence effects in JUNO would indicate that our understanding of the coherence of neutrino sources is, at least, incomplete.

# Coherent Elastic Neutrino-Nucleus Scattering (CEνNS) and Neutrino Generalized Interactions

D. Aristizabal, VDR, N. Rojas, Phys.Rev. D98 (2018) 075018

# Observation of CEνNS at COHERENT (2017)

NEUTRINO PHYSICS

## Observation of coherent elastic neutrino-nucleus scattering

D. Akimov,[1,2] J. B. Albert,[3] P. An,[4] C. Awe,[4,5] P. S. Barbeau,[4,5] B. Becker,[6] V. Belov,[1,2] A. Brown,[4,7] A. Bolozdynya,[2] B. Cabrera-Palmer,[8] M. Cervantes,[5] J. I. Collar,[9]* R. J. Cooper,[10] R. L. Cooper,[11,12] C. Cuesta,[13]† D. J. Dean,[14] J. A. Detwiler,[13] A. Eberhardt,[13] Y. Efremenko,[6,14] S. R. Elliott,[12] E. M. Erkela,[13] L. Fabris,[14] M. Febbraro,[14] N. E. Fields,[9]‡ W. Fox,[3] Z. Fu,[13] A. Galindo-Uribarri,[14] M. P. Green,[4,14,15] M. Hai,[9]§ M. R. Heath,[3] S. Hedges,[4,5] D. Hornback,[14] T. W. Hossbach,[16] E. B. Iverson,[14] L. J. Kaufman,[3]|| S. Ki,[4,5] S. R. Klein,[10] A. Khromov,[2] A. Konovalov,[1,2,17] M. Kremer,[4] A. Kumpan,[2] C. Leadbetter,[4] L. Li,[4,5] W. Lu,[14] K. Mann,[4,15] D. M. Markoff,[4,7] K. Miller,[4,5] H. Moreno,[11] P. E. Mueller,[14] J. Newby,[14] J. L. Orrell,[16] C. T. Overman,[16] D. S. Parno,[13]¶ S. Penttila,[14] G. Perumpilly,[9] H. Ray,[18] J. Raybern,[5] D. Reyna,[8] G. C. Rich,[4,14,19] D. Rimal,[18] D. Rudik,[1,2] K. Scholberg,[5] B. J. Scholz,[9] G. Sinev,[5] W. M. Snow,[3] V. Sosnovtsev,[2] A. Shakirov,[2] S. Suchyta,[10] B. Suh,[4,5,14] R. Tayloe,[3] R. T. Thornton,[3] I. Tolstukhin,[3] J. Vanderwerp,[3] R. L. Varner,[14] C. J. Virtue,[20] Z. Wan,[4] J. Yoo,[21] C.-H. Yu,[14] A. Zawada,[4] J. Zettlemoyer,[3] A. M. Zderic,[13] COHERENT Collaboration#

The coherent elastic scattering of neutrinos off nuclei has eluded detection for four decades, even though its predicted cross section is by far the largest of all low-energy neutrino couplings. This mode of interaction offers new opportunities to study neutrino properties and leads to a miniaturization of detector size, with potential technological applications. We observed this process at a 6.7$\sigma$ confidence level, using a low-background, 14.6-kilogram CsI[Na] scintillator exposed to the neutrino emissions from the Spallation Neutron Source at Oak Ridge National Laboratory. Characteristic signatures in energy and time, predicted by the standard model for this process, were observed in high signal-to-background conditions. Improved constraints on nonstandard neutrino interactions with quarks are derived from this initial data set.


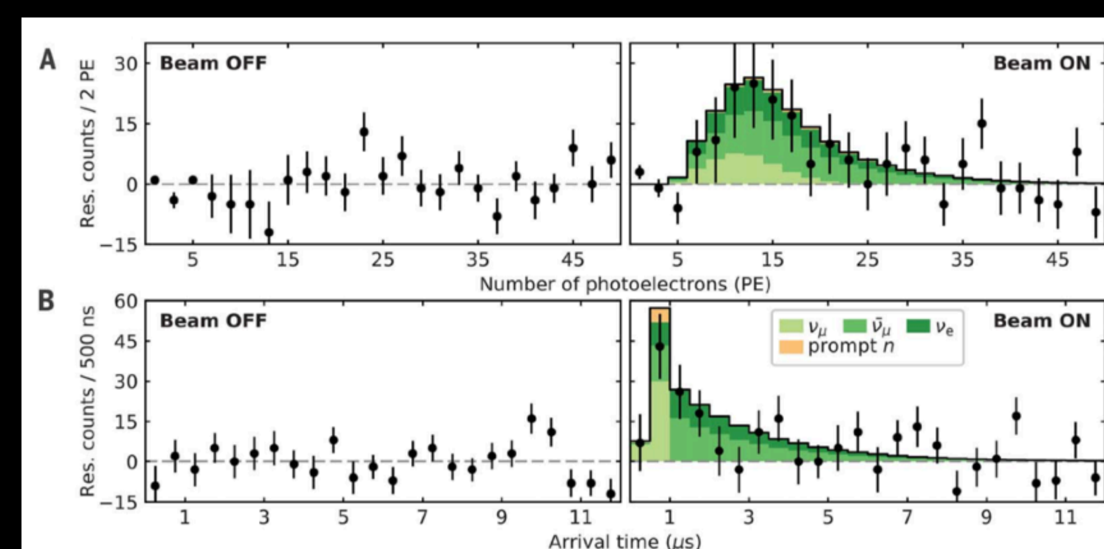


Akimov et al., Science 357, 1123–1126 (2017)

# Coherent Elastic Neutrino-Nucleus Scattering

- NC (flavour-independent) process: $\nu + A \rightarrow \nu + A$

- CE$\nu$NS occurs when the neutrino energy $E_\nu$ is such that nucleon amplitudes sum up coherently (up to $E_\nu$ ~ 100 MeV):
  cross section enhancement

- Total cross section scales approximately like $N^2$

$$\frac{d\sigma}{dE_R} \propto N^2$$

- Can be few orders of magnitude larger than inverse beta decay process used to first observe neutrinos

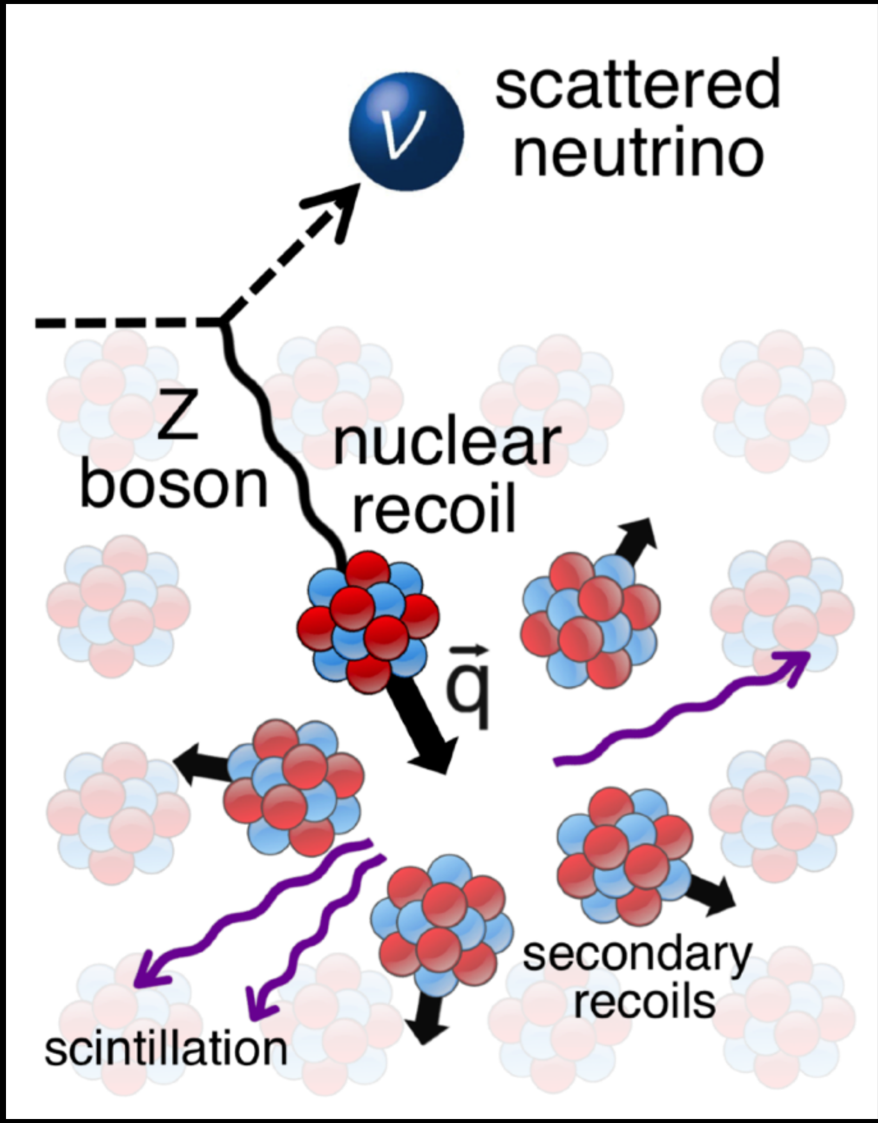


Image from COHERENT exp.

D.Z. Freedman, Phys. Rev. D 9 (1974)
V.B. Kopeliovich and L.L. Frankfurt, ZhETF Pis. Red. 19 (1974)

# Coherent Elastic Neutrino-Nucleus Scattering

CEνNS has a well-calculable cross-section in the SM

Nuclear Form Factor

$$\frac{d\sigma_{\rm coh}}{dT} = \frac{G_F^2}{4\pi} M Q_W^2 \left(1 - \frac{MT}{2E_\nu^2}\right) F_{\rm nucl}^2(Q^2)$$

$$Q_W = \left[Z(1 - 4\sin^2\theta_W) - N\right]$$

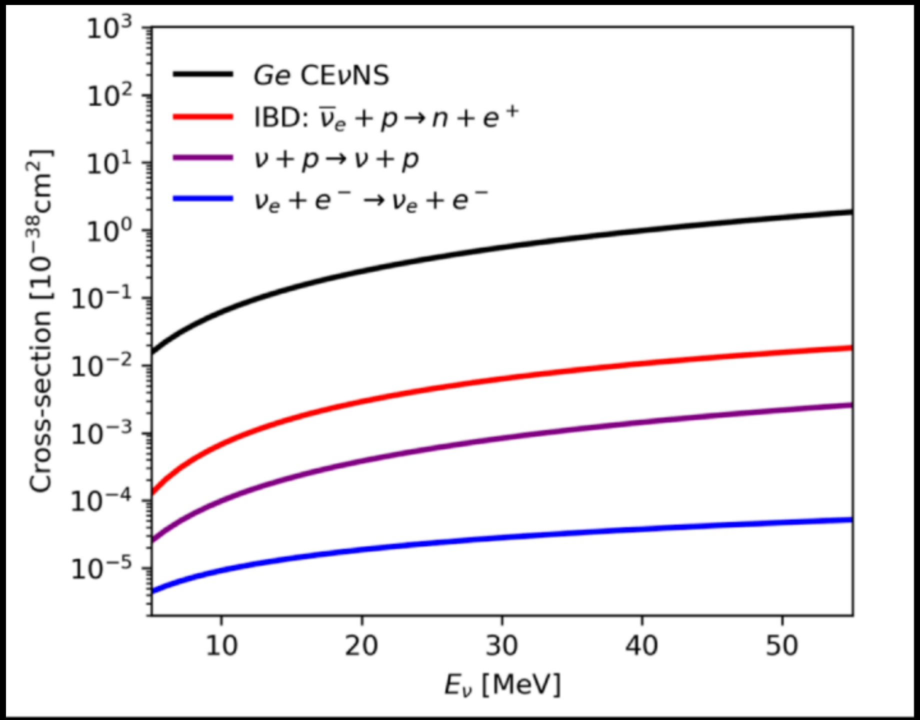


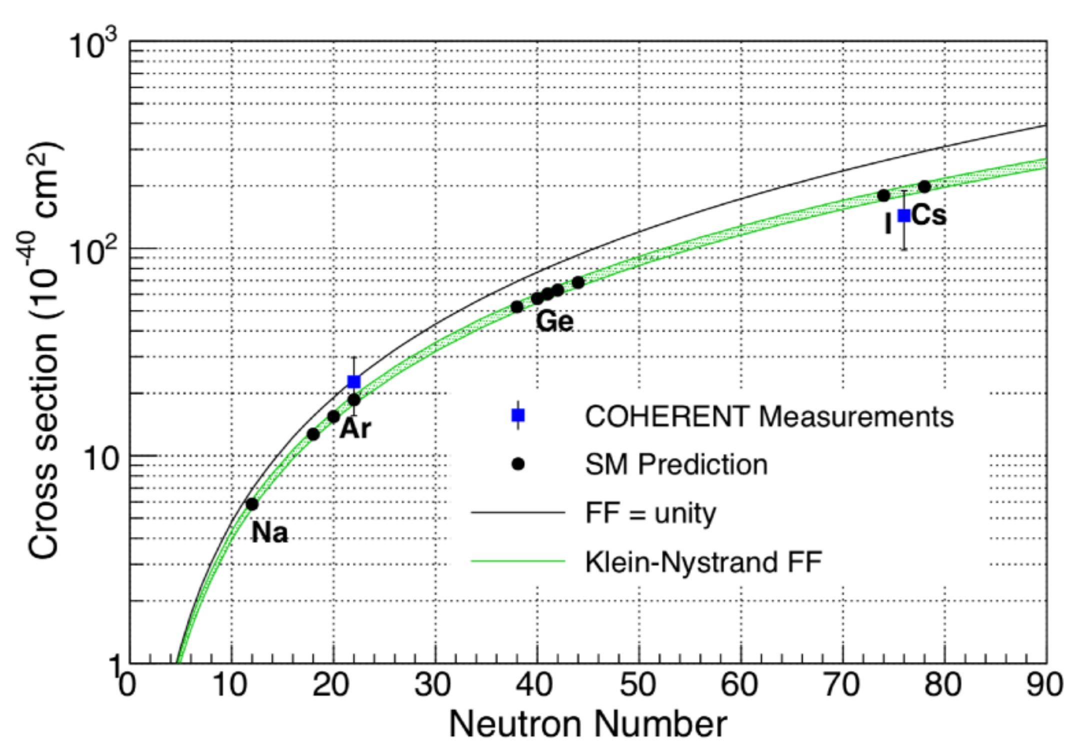


Credit to J. Newby @Neutrino 2020

Akimov et al., Science 357, 1123–1126 (2017)
Akimov et al., 2003.10630, 2006.12659

# Coherent Elastic Neutrino-Nucleus Scattering

- CEνNS is an exceptionally challenging process to observe
- Despite its large cross section, not observed for years due to tiny nuclear recoil energies
  - Heavier nuclei: higher cross section but lower recoil
  - Both cross-section and maximum recoil energy increase with neutrino energy
  - Max recoil energy: $E_R^{\max} = \frac{2E_\nu^2}{m_N}$

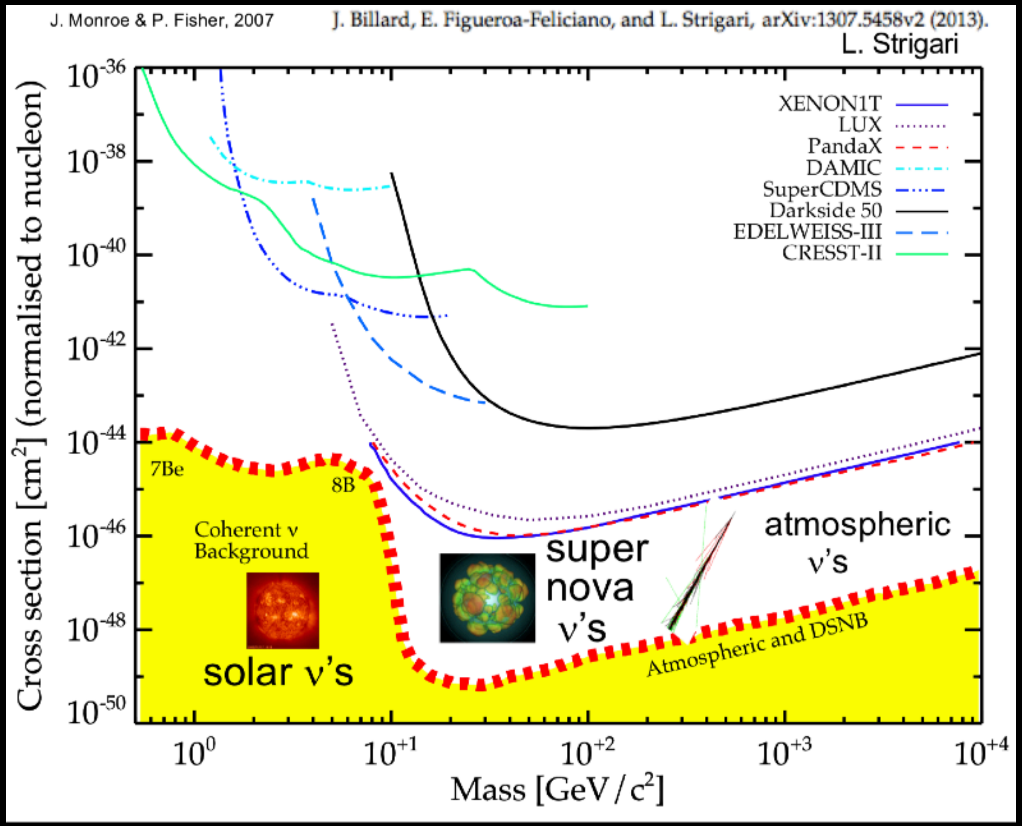


- Related to dark matter direct detection experiments:
  - CEνNS from natural neutrinos creates ultimate background for direct DM search experiments

D.Z. Freedman, Phys. Rev. D 9 (1974)
M.W. Goodman, E. Witten, Phys Rev D 31 (1985)
Billard et al., Phys. Rev. D89 (2014) 023524

# The COHERENT experiment

- COHERENT collaboration observed CEνNS at a 6.7-sigma confidence level in 2017 (more than 40 years after its prediction)
- Uses intense neutrino source provided by Spallation Neutron Source (SNS) at Oak Ridge National Laboratory
- (~1 GeV) Pulsed protons hit a liquid mercury fixed target
- Neutrinos stem from the decays of stopped pions and muons resulting in flux with well-defined spectral and timing characteristics

$$\pi^+ \rightarrow \mu^+ + \nu_\mu$$ monochromatic, prompt

$$\mu^+ \rightarrow e^+ + \nu_e + \bar{\nu}_\mu$$ delayed

- The COHERENT detector uses different nuclear targets to allow for measurement of characteristic $N^2$ cross-section dependence
- First observation made with 14.6 kg of CsI[Na]

Akimov et al., Science (2017), 1708.01294
Asimov et. al, 1804.09459
K. Scholberg, Phys. Rev. D73 (2006) 033005

# CEνNS physics potential

- CEvNS opens the window to a rich neutrino physics programme
  - Supernovae physics: determination of SN neutrino properties through measurement of the neutrino DSNB or neutrino emission in a single SN explosion
  - Nuclear properties such as: neutron form factor, neutron radius …
  - Measurement, study and test of the SM axial nuclear current
  - Fundamental neutrino physics (weak mixing angle, effective neutrino charge radius and magnetic moment …)

- New physics such as: non-standard neutrino interactions, sterile neutrinos, new NC heavy or light mediators …

- COHERENT measurement consistent with SM at 1σ

- Still open room for new physics

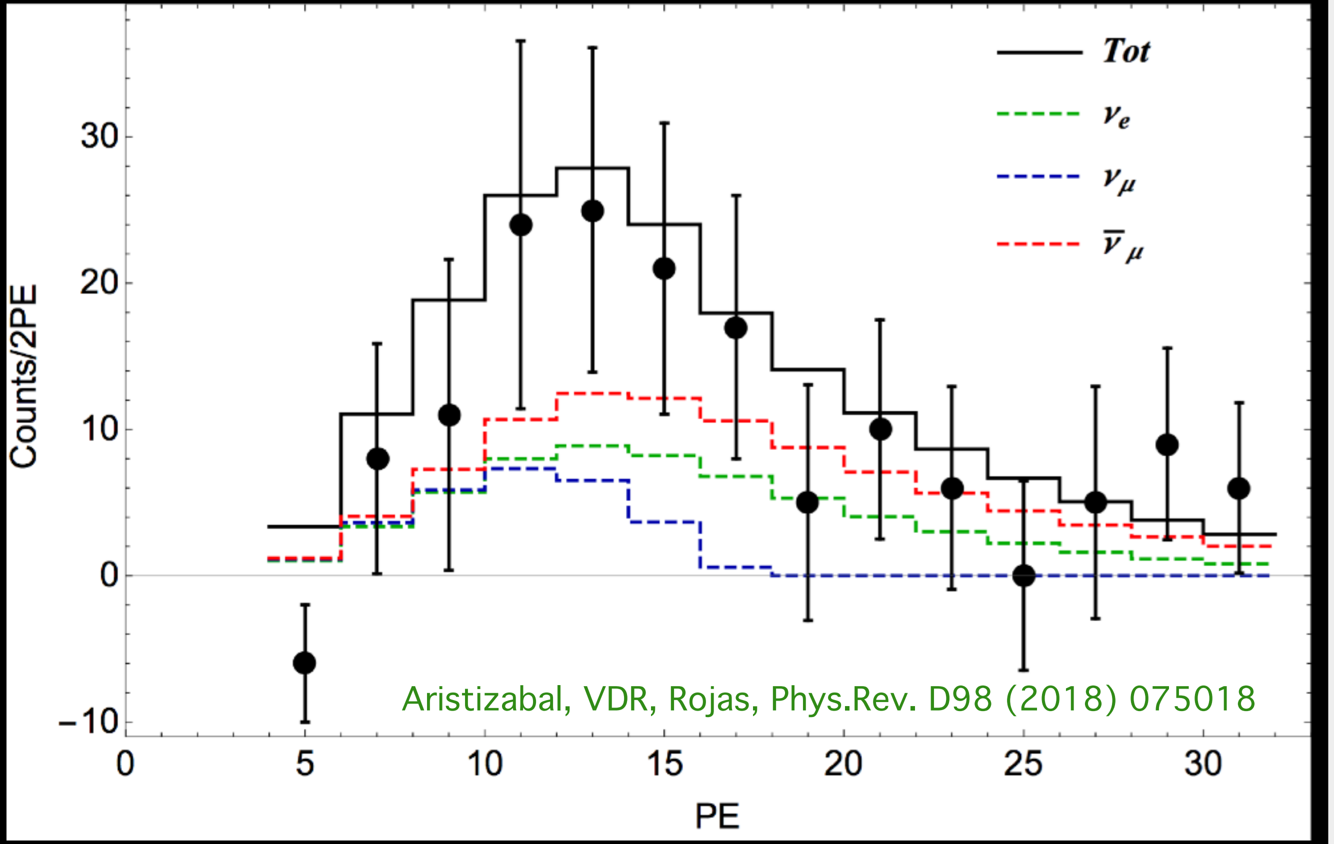



D.Z. Freedman, Phys. Rev. D 9 (1974), C. Horowitz et al., Phys. Rev. D 68 (2003), H. Davoudiasl et al., Phys. Rev. D 89 (2014), J. Barranco et al., Phys. Rev. D 76 (2007), K. Patton et al., Phys. Rev. C 86 (2012), C. Horowitz & J. Piekarewicz, Phys. Rev. Lett. 86 (2000), K. Scholberg, Phys. Rev. D 73 (2006), P. Coloma et al., Phys. Rev. D 96 (2017), A.J. Anderson et al., Phys. Rev. D 86 (2012), Coloma et al. Phys. Rev. D 96, 115007, Cadeddu et al Phys. Rev. Lett. 120, 072501, Liao and Marfatia Phys. Lett. B775 (2017) 54–57, Papoulias and Kosmas Phys. Rev. D97 (2018) 033003, Farzan et al. JHEP 05 (2018) 066, …

# CEνNS and new physics interactions

- Neutrino NSI: non-standard interactions parametrised in a model-independent and phenomenological way

$$\mathcal{L} \sim G_F \sum_{q=u,d} \bar{\nu}_i (1-\gamma_5)\gamma_\mu \nu_j \bar{q}(\epsilon_{ij}^{qV} - \epsilon_{ij}^{qA}\gamma_5)\gamma^\mu q$$

- Pheno constraints from forward coherent scattering (matter potentials), DIS and oscillation data, LHC mono jet …

Coloma et al. Phys. Rev. D 96, 115007, Gonzalez-Garcia et al. 1803.03650

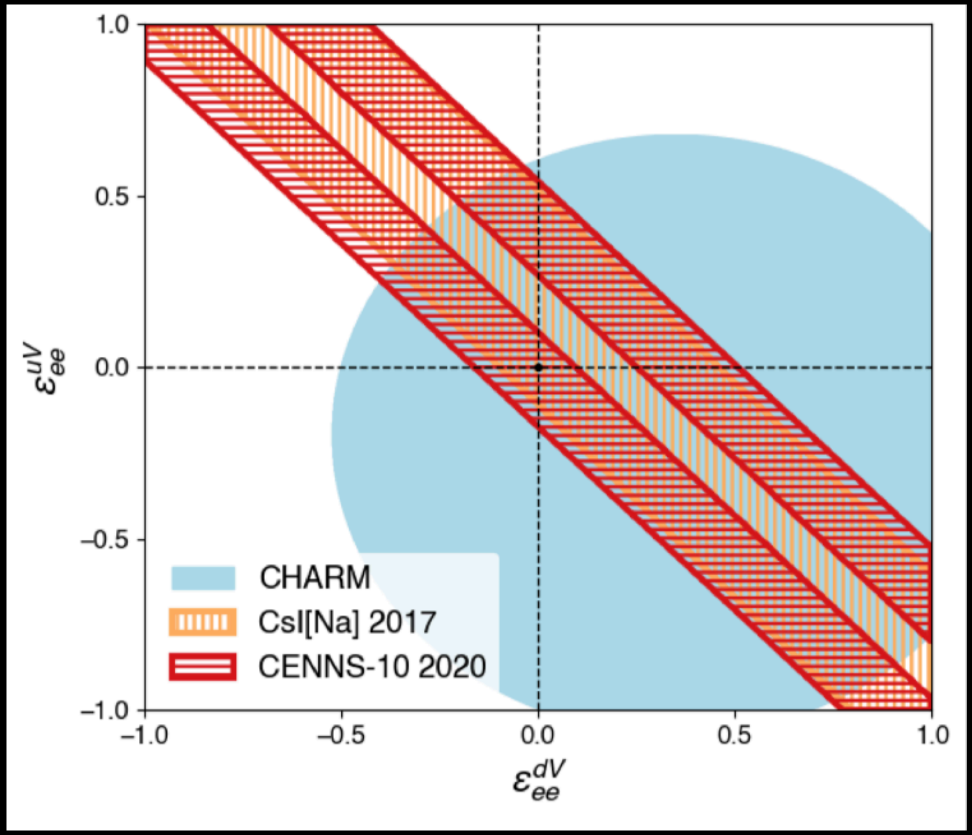


COHERENT collab. arXiv:2003.10630

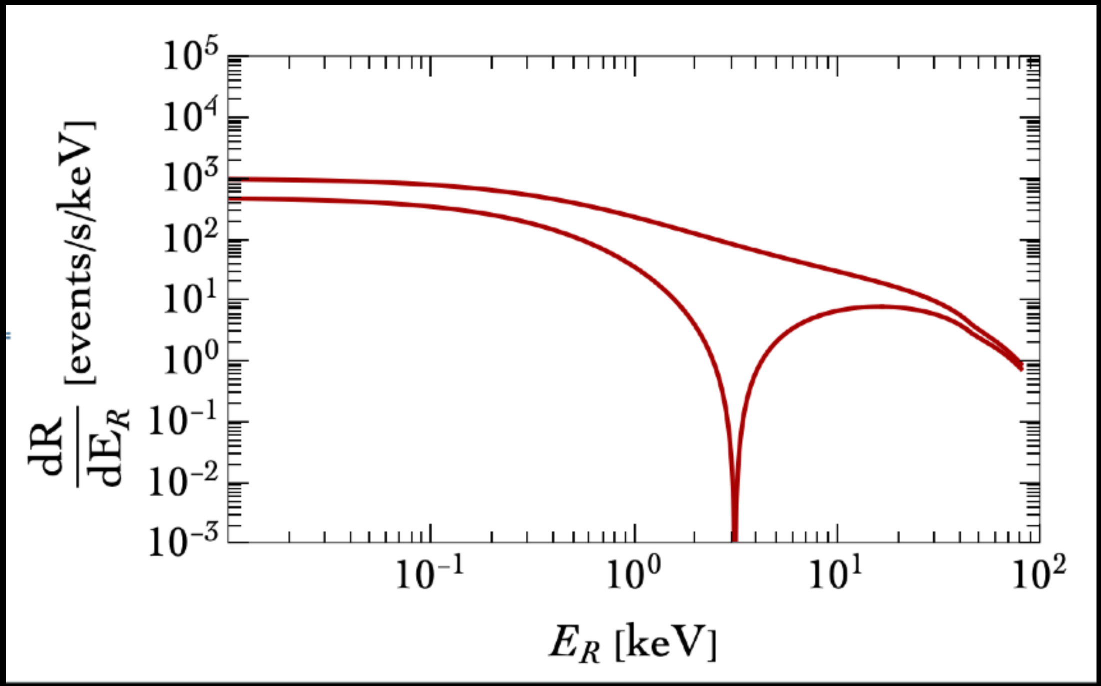


Aristizabal, VDR, Rojas JHEP 1909 (2019) 069

# Neutrino Generalised Interactions (NGI)

- NSI are a subset of a larger set of neutrino-quark interactions: Neutrino Generalized Interactions (NGI)
- all Lorentz invariant non-derivative interactions of neutrinos with first generation quarks

$$\mathscr{L}_{\text{eff}}^{\text{NGI}} = \frac{G_F}{\sqrt{2}} \sum_X \bar{\nu}\Gamma^X \nu \, \bar{q}\Gamma_X \left(C_X^q + i\gamma_5 D_X^q\right) q$$

Kayser et al. Phys. Rev. D 20, 87
Lindner et al. JHEP03(2017)097

$$\Gamma_X = \{\mathbb{I}, i\gamma_5, \gamma_\mu, \gamma_5\gamma_\mu, \sigma_{\mu\nu}\}$$

$$\mathscr{L}_S \sim (\bar{\nu}\nu)\left[\bar{q}\left(C_S^q + i\gamma_5 D_S^q\right) q\right]$$

$$\mathscr{L}_P \sim (\bar{\nu}\gamma_5\nu)\left[\bar{q}\left(\gamma_5 C_P^q + i D_P^q\right) q\right]$$

$$\mathscr{L}_V \sim (\bar{\nu}\gamma^\mu\nu)\left[\bar{q}\left(\gamma_\mu C_V^q + i\gamma_\mu\gamma_5 D_V^q\right) q\right]$$

$$\mathscr{L}_A \sim (\bar{\nu}\gamma^\mu\gamma_5\nu)\left[\bar{q}\left(\gamma_\mu\gamma_5 C_A^q + i\gamma_\mu D_A^q\right) q\right]$$

$$\mathscr{L}_T \sim (\bar{\nu}\sigma^{\mu\nu}\nu)\left[\bar{q}\left(\sigma_{\mu\nu} C_T^q + i\sigma_{\mu\nu}\gamma_5 D_T^q\right) q\right]$$

- Constrain dominant spin-independent contributions ($C^q_X$)
- Neglect Pseudoscalar and Axial interactions (spin-dependent: $Z_\uparrow - Z_\downarrow$, $N_\uparrow - N_\downarrow$)

Freedman et al. Ann. Rev. Nucl. Part. Sci. 27 (1977)

# NGI and CEvNS

- Cross section parameterised in terms of nuclear currents: Scalar, Vector and Tensor

$$\frac{d\sigma^a(q^2=0)}{dE_r} = \frac{G_F^2}{4\pi} m_{N_a} N_a^2 \left[ \xi_S^2 \frac{E_r}{E_r^{\text{max}}} + \xi_V^2 \left(1 - \frac{E_r}{E_r^{\text{max}}} - \frac{E_r}{E_\nu}\right) + \xi_T^2 \left(1 - \frac{E_r}{2E_r^{\text{max}}} - \frac{E_r}{E_\nu}\right) - R\frac{E_r}{E_\nu} \right]$$

$$E_r^{\max} \simeq 2E_\nu^2/m_{N_a}$$

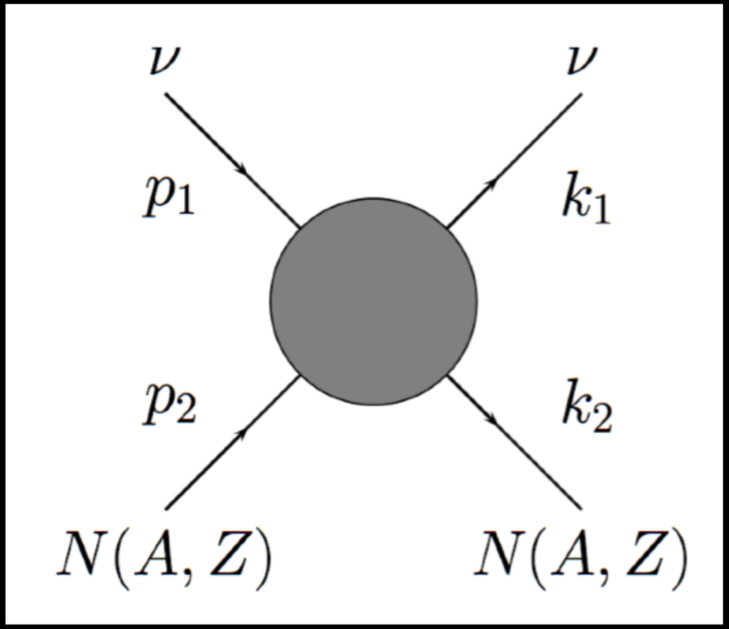


- Single-parameter scenario
- Two-parameter scenario


Lindner et al. JHEP03(2017)097
D. Aristizabal, VDR, N. Rojas, Phys.Rev. D98 (2018) 075018

# COHERENT constraints on NGI

$$\chi^2 = \sum_{i=4}^{16} \left( \frac{N_i^{\text{meas}} - (1+\alpha) N_i^{\text{NGI}}(\mathscr{P}) - (1+\beta) B_i^{\text{on}}}{\sigma_i} \right)^2 + \left( \frac{\alpha}{\sigma_\alpha} \right)^2 + \left( \frac{\beta}{\sigma_\beta} \right)^2$$

- Single-parameter scenario
- Constraints on scalar-type interactions are the most stringent

| Param | BFP value | 90% CL | 99% CL |
|---|---|---|---|
| $\xi_S$ | 0 | $[-0.62, 0.62]$ | $[-1.065, 1.065]$ |
| $\xi_V$ | $-0.113$ | $[-0.324, 0.224]$ | $[-0.436, 0.67]$ |
| | $-1.764$ | $[-2.102, -1.554]$ | $[-2.545, -1.442]$ |
| $\xi_T$ | 0 | $[-0.591, 0.591]$ | $[-1.071, 1.072]$ |

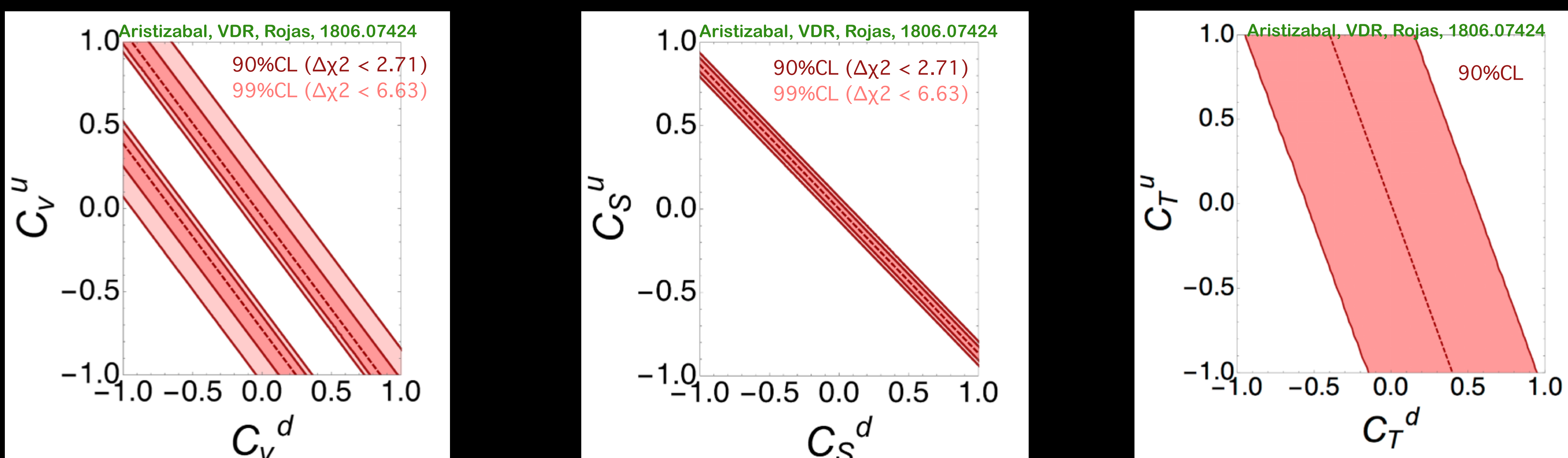

# COHERENT constraints on NGI

- Two-parameter scenario

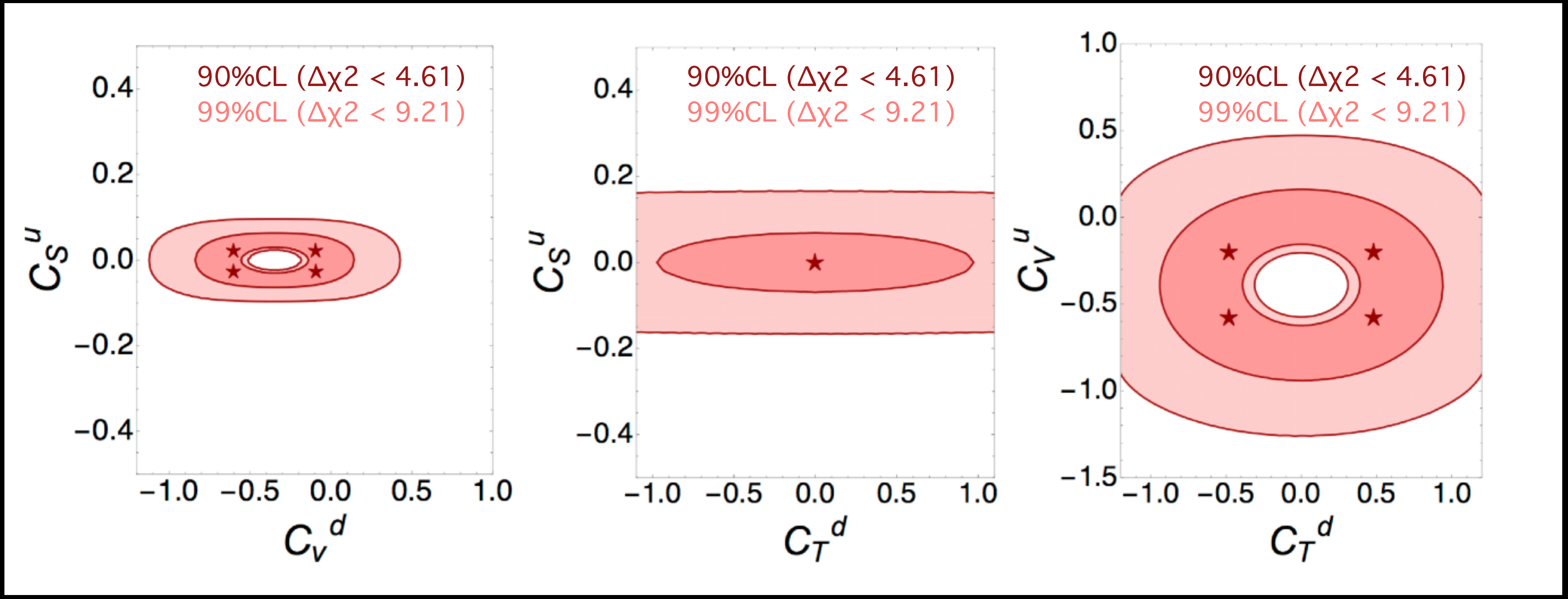


- The presence of an additional interaction at the nuclear level relaxes the bounds on the fundamental neutrino-quark couplings

$$\xi_V = -C_V = -[1 - (1 - 4\sin^2\theta_w) - N/Z] \simeq -0.95$$

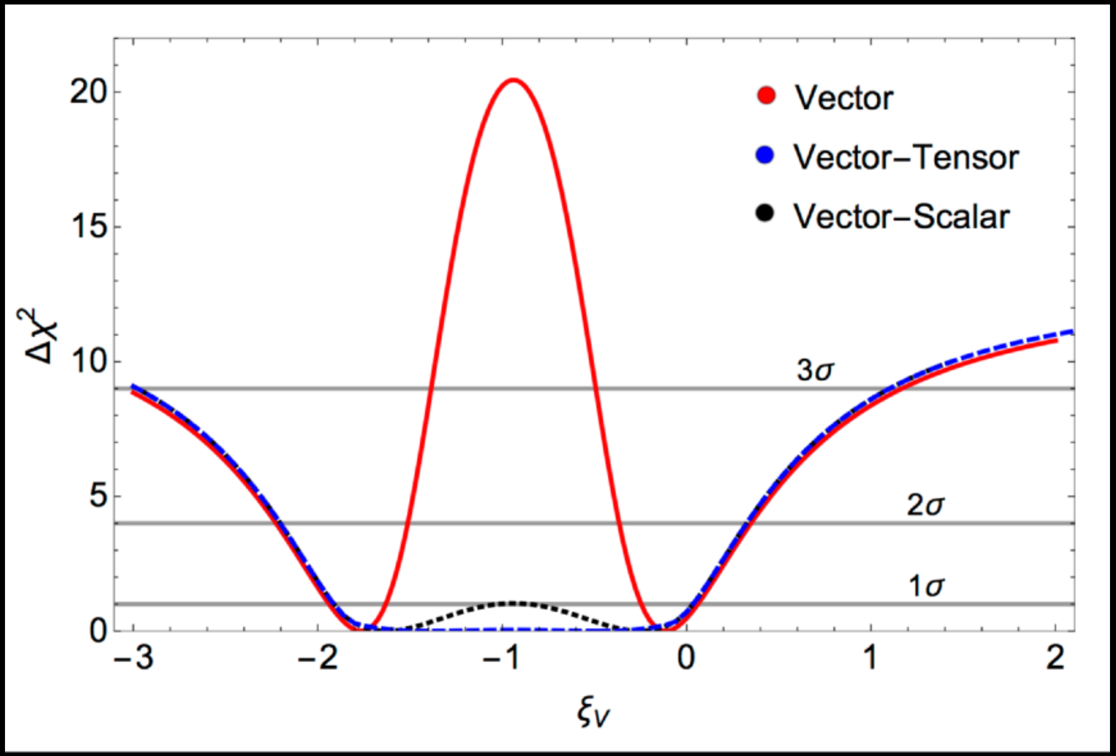

# Summary of CEνNS constraints on NGI

- We have studied a generic set of effective Lorentz invariant non-derivative neutrino-quark interactions (NGI).
- We have employed the recent COHERENT data to place constraints on the different NGI effective parameters.
- In the single-parameter case, our findings show that the scalar interaction is the most constrained, with the tightest bound found for the Lorentz mixed pseudoscalar-scalar coupling.
- In the two-parameter case, we have found that the presence of an additional interaction at the nuclear level relaxes the bounds on the fundamental neutrino-quark couplings.
- CEνNS offers a plethora of physics opportunities. Forthcoming data from COHERENT and reactor experiments will allow unraveling the presence of new physics.


Thank you!
Standard Model

# Backup

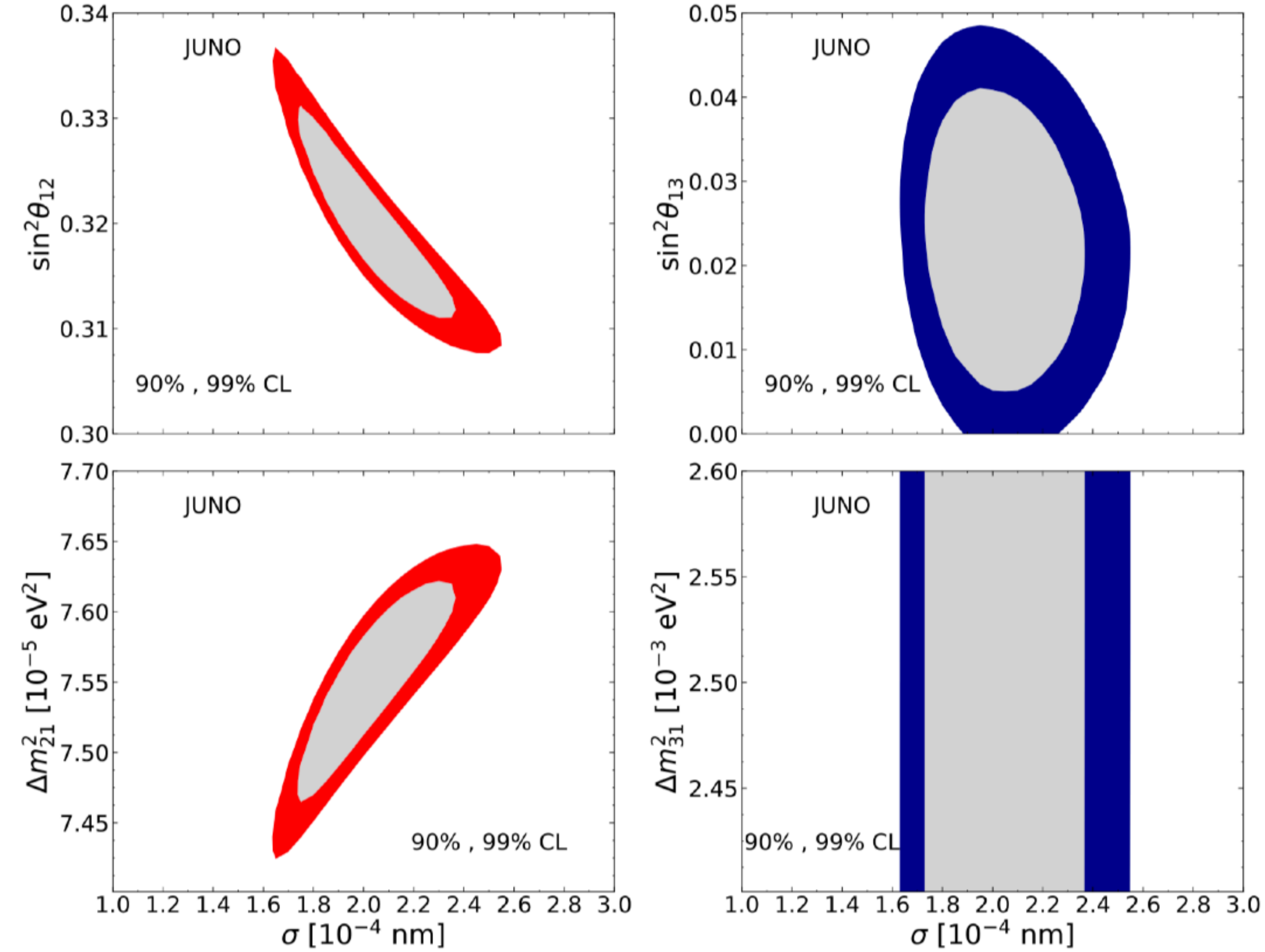


FIG. 7: 90 and 99% CL (2 d.o.f.) allowed regions in the $\sigma$–$\sin^2\theta_{12}$ (top,left), $\sigma$–$\Delta m^2_{21}$ (bottom,left), $\sigma$–$\sin^2\theta_{13}$ (top,right), and $\sigma$–$\Delta m^2_{31}$ (bottom, right) planes, obtained by analyzing simulated JUNO data consistent with strong decoherence ($\sigma = 2.01 \times 10^{-4}$ nm). The input values for the standard solar oscillation parameters are listed in Eqs. (5) while $\Delta m^2_{31} = 2.63 \times 10^{-3}$ eV$^2$ and $\sin^2\theta_{13} = 0.0231$. See text for details.

There is no sensitivity to $\Delta m_{31}$. Long-wavelength effects are still present and hence both $\Delta m^2_{21}$ and $\sin^2\theta_{12}$ can be measured. Similar to what we observe for RENO and Daya Bay, measurements of the oscillation frequency and amplitude are strongly correlated with those of σ. Smaller sigma translate into larger $\sin^2\theta_{12}$ in order to compensate for the flattened-out oscillation probability while smaller sigma translate into smaller $\Delta m^2_{21}$ in order to compensate for the shift of the oscillation maximum to larger energies (smaller L/E). These degeneracies lead to a less precise determination of the solar parameters.

# Coherent Elastic Neutrino-Nucleus Scattering

CEνNS has a well-calculable cross-section in the SM

$$\frac{d\sigma_{coh}}{dT} = \frac{G_F^2 M}{2\pi}\left[(G_V + G_A)^2 + (G_V - G_A)^2 \times \left(1 - \frac{T}{E_\nu}\right)^2 - (G_V^2 - G_A^2)\frac{MT}{E_\nu^2}\right],$$

$$G_V = (g_V^p Z + g_V^n N) F_{nucl}^V(Q^2),$$

$$G_A = \left(g_A^p (Z_+ - Z_-) + g_A^n (N_+ - N_-)\right) F_{nucl}^A(Q^2)$$

T: recoil energy

$Z_\pm$ $N_\pm$ : number or protons and neutrons with opposite spins

$F_{nucl}$: nuclear form factors (close to 1 at low $Q^2$)

For heavy nuclei the axial contribution is small because is determined only by unpaired protons and neutrons.

D.Z. Freedman, Phys. Rev. D 9 (1974)
V.B. Kopeliovich and L.L. Frankfurt, ZhETF Pis. Red. 19 (1974)

# CEvNS experiments worldwide

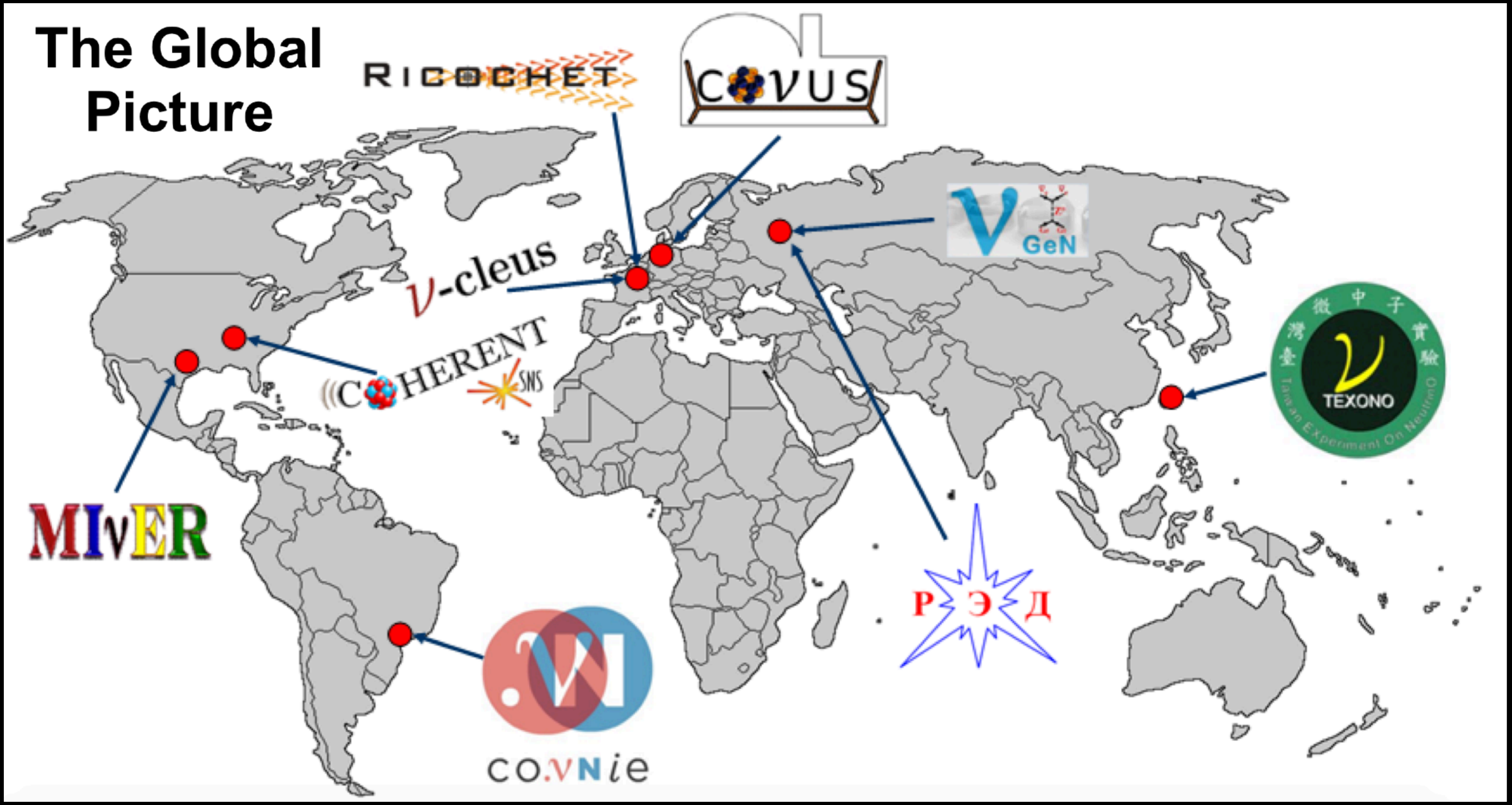


Credit to M. Green @Aspen 2019 Winter Conference

# CEvNS status

From accelerators:

- The COHERENT detector uses different nuclear targets to allow for measurement of characteristic $N^2$ cross-section dependence
- Recent result LAr result: CEvNS preference over the background-only null hypothesis with greater than 3σ significance.

| Nuclear Target | Technology | Mass (kg) | Distance from source (m) | Recoil threshold (keVr) | Data-taking start date | Future |
|---|---|---|---|---|---|---|
| CsI[Na] | Scintillating crystal | 14.6 | 20 | 6.5 | 9/2015 | Decommissioned |
| Ge | HPGe PPC | 16 | 20 | <few | 2020 | Funded by NSF MRI, in progress |
| LAr | Single-phase | 22 | 20 | 20 | 12/2016, upgraded summer 2017 | Expansion to **750 kg scale** |
| NaI[Tl] | Scintillating crystal | 185*/ 3388 | 28 | 13 | *high-threshold deployment summer 2016 | Expansion to **3.3 tonne**, up to 9 tonnes |

Credit to K. Scholberg @ TAUP 2019

From nuclear reactors:

- Anti_ve are produced in fission reactions (single flavor); recoil energies<keV and backgrounds make it very challenging. E.g. CONUS, TEXONO, CONNIE, νCLEUS…

| Source | Flux/ ν's per s | Flavor | Energy | Pros | Cons |
|---|---|---|---|---|---|
| **Reactor** | 2e20 per GW | nuebar | few MeV | • huge flux | • lower xscn<br>• require very low threshold<br>• CW |
| **Stopped pion** | 1e15 | numu/ nue/ nuebar | 0-50 MeV | • higher xscn<br>• higher energy recoils<br>• pulsed beam for bg rejection<br>• multiple flavors | • lower flux<br>• potential fast neutron in-time bg |

Credit to K. Scholberg @ TAUP 2019


Akimov et al., Science (2017), 1708.01294
Akimov et. al, 1804.09459
Akimov et al. 1909.05913
K. Scholberg, Phys. Rev. D73 (2006) 033005
Aguilar-Arevalo et al. 1906.02200
COHERENT collab. arXiv:2003.10630

# From quark to nuclear currents

- To compute the CEνNS cross section induced by the NGI we assume a fermion nuclear ground state with spin J = 1/2.

$$\frac{d\sigma^a(q^2=0)}{dE_r} = \frac{G_F^2}{4\pi} m_{N_a} N_a^2 \left[ \xi_S^2 \frac{E_r}{E_r^{\text{max}}} + \xi_V^2 \left(1 - \frac{E_r}{E_r^{\text{max}}} - \frac{E_r}{E_\nu}\right) + \xi_T^2 \left(1 - \frac{E_r}{2E_r^{\text{max}}} - \frac{E_r}{E_\nu}\right) - R \frac{E_r}{E_\nu} \right]$$

$$\xi_S^2 = \frac{C_S^2 + D_P^2}{N^2}, \quad \xi_V^2 = \frac{C_V^2 + D_A^2}{N^2}, \quad \xi_T^2 = 8\frac{C_T^2}{N^2}, \quad R = 2\frac{C_S C_T}{N^2}$$

$$E_r^{\text{max}} \simeq 2E_\nu^2/m_{N_a}$$

- ν – N coefficients are written as follows

$$C_S = Z \sum_{q=u,d} C_S^{(q)} \frac{m_p}{m_q} f_{T_q}^p + (A-Z) \sum_{q=u,d} C_S^{(q)} \frac{m_n}{m_q} f_{T_q}^n ,$$

$$C_V = Z\left(2C_V^u + C_V^d\right) + (A-Z)\left(C_V^u + 2C_V^d\right) ,$$

$$C_T = Z\left(\delta_u^p C_T^u + \delta_d^p C_T^d\right) + (A-Z)\left(\delta_u^n C_T^u + \delta_d^n C_T^d\right) .$$

e.g. Dent et al. Phys. Rev. D92 (2015) 063515

# From quark to nuclear currents

- To compute the CEνNS cross section induced by the NGI we assume a fermion nuclear ground state with spin J = 1/2.

$$\frac{d\sigma^a(q^2=0)}{dE_r} = \frac{G_F^2}{4\pi} m_{N_a} N_a^2 \left[\xi_S^2 \frac{E_r}{E_r^{\text{max}}} + \xi_V^2 \left(1 - \frac{E_r}{E_r^{\text{max}}} - \frac{E_r}{E_\nu}\right) + \xi_T^2 \left(1 - \frac{E_r}{2E_r^{\text{max}}} - \frac{E_r}{E_\nu}\right) - R\frac{E_r}{E_\nu}\right]$$

- STEP I: $\mathcal{O}_q \xrightarrow{\text{step (I)}} \mathcal{O}_n$ we calculate quark currents in nucleons according to

e.g. Dent et al. Phys. Rev. D

$$\langle n(p_f)|\bar{q}\,q|n(p_i)\rangle = \frac{m_n}{m_q} f_{T_q}\,\bar{n}\,n\,,$$

$$\langle n(p_f)|\bar{q}\gamma^\mu q|n(p_i)\rangle = \mathcal{N}_q^n\,\bar{n}\,\gamma^\mu\,n\,,$$

$$\langle n(p_f)|\bar{q}\,\sigma^{\mu\nu}\,q|n(p_i)\rangle = \delta_q^n\,\bar{n}\,\sigma^{\mu\nu}\,n\,.$$

- STEP II: $\mathcal{O}_n \xrightarrow{\text{step (II)}} \mathcal{O}_N$ we evaluate the correlators of nucleonic currents in nuclei, which involve nuclear form factors:

$$\langle N(k_2)|\bar{n}\,n|N(p_2)\rangle = \bar{N}\,N F(q^2)$$

Helm form factor

$$\langle N(k_2)|\bar{n}\gamma^\mu n|N(p_2)\rangle = \bar{N}\left(\gamma^\mu F(q^2) + \frac{\sigma^{\mu\nu}q_\nu}{2m_N}F_1(q^2)\right)N$$

$$\langle N(k_2)|\bar{n}\,\sigma^{\mu\nu}\,n|N(p_2)\rangle = \bar{N}\left(i\sigma^{\mu\nu}F(q^2) - \frac{\gamma^\mu q^\nu - \gamma^\nu q^\mu}{2m_N}F_2(q^2) - \frac{K^\mu q^\nu - K^\nu q^\mu}{2m_N^2}F_3(q^2)\right)N$$

# CEνNS and new light mediators

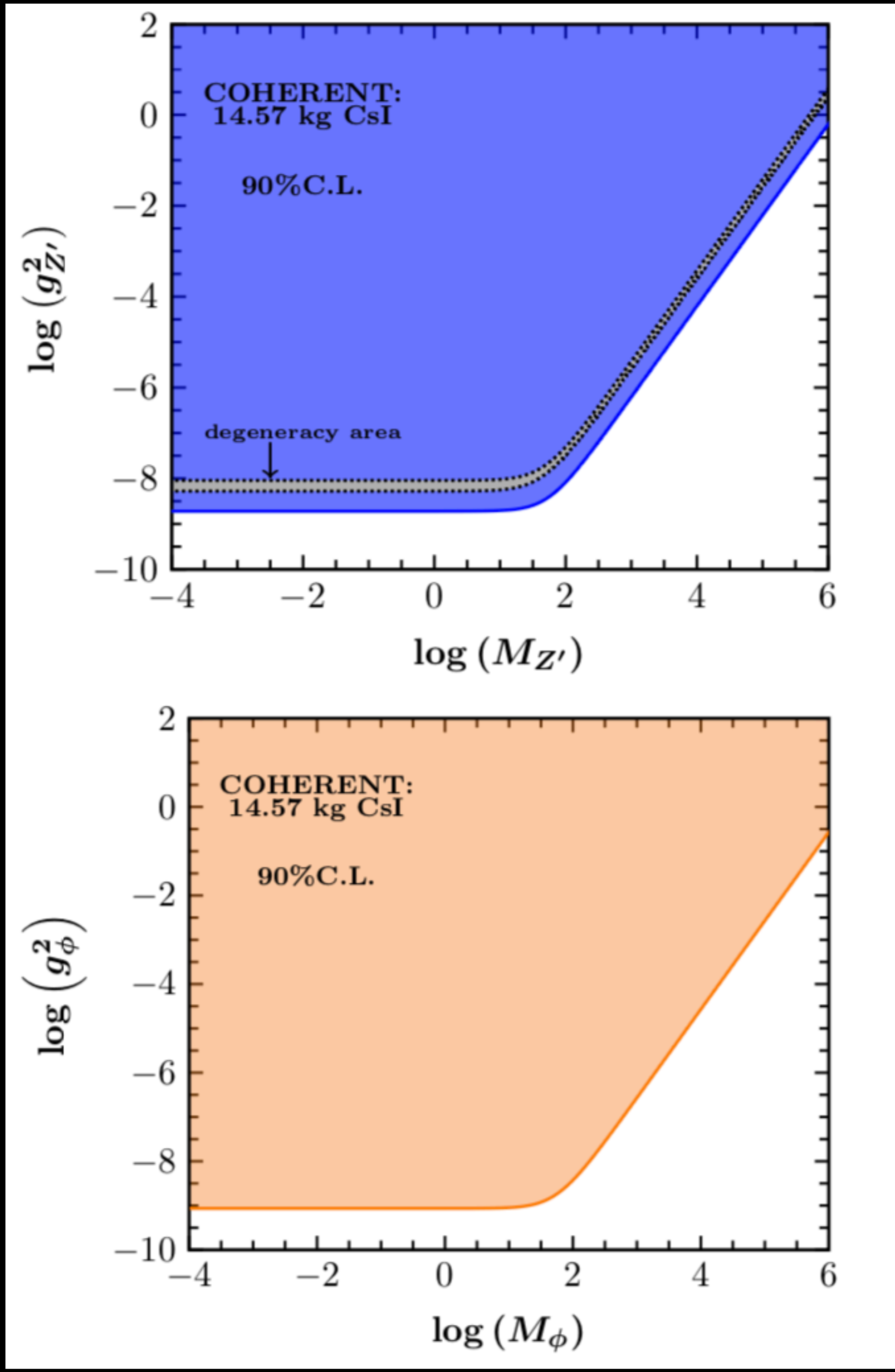


Papoulias and Kosmas, Phys.Rev. D97 (2018) 033003

$$\mathcal{L}_{\rm vec} = Z'_\mu \left( g^{qV}_{Z'}\, \bar{q}\gamma^\mu q + g^{\nu V}_{Z'}\, \bar{\nu}_L \gamma^\mu \nu_L \right) + \frac{1}{2} M^2_{Z'} Z'_\mu Z'^\mu \,.$$

$$\mathcal{L}_{\rm sc} = \phi \left( g^{qS}_{\phi}\, \bar{q}q + g^{\nu S}_{\phi}\, \bar{\nu}_R \nu_L + {\rm H.c.} \right) - \frac{1}{2} M^2_{\phi} \phi^2$$

See also:
Liao et al. PLB 775 (2017)
Abdullah et al. PRD98 (2018) 015005
Dutta et al. PRD 93 (2016) 013015

# COHERENT constraints on NGI

- Single-parameter scenario
- Sizeable NGI (vector interactions) are allowed

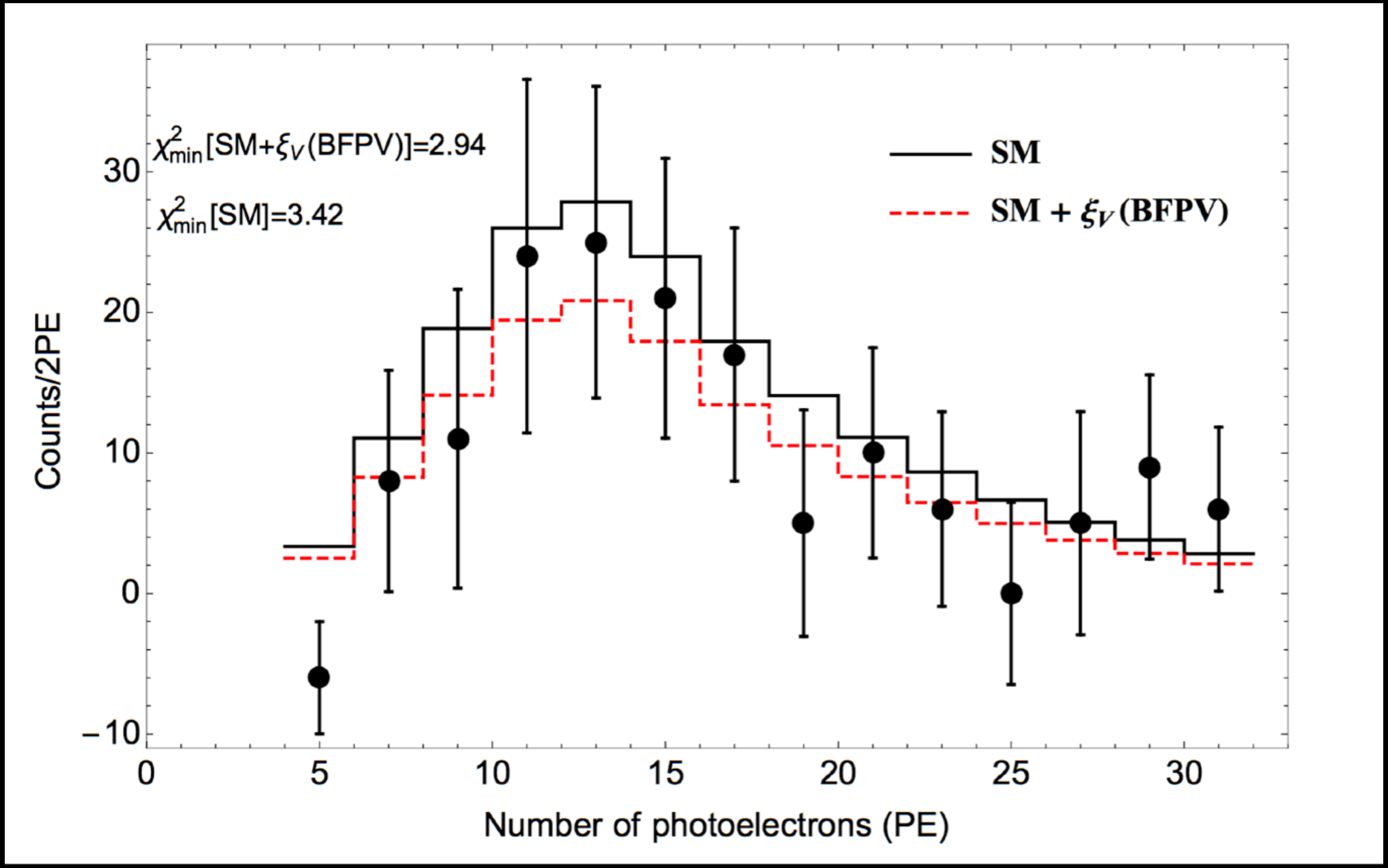


$n_{PE} = 1.17 (E_R/\text{keV})$